UNIVERSITÉ DU QUÉBEC À MONTRÉAL

CHARACTERIZATION AND *IN VIVO* NUCLEAR MAGNETIC RESONANCE STUDY OF THE BACTERIUM *AEROMONAS SALMONICIDA* RESPONSIBLE FOR FURUNCULOSIS IN SALMONIDS

THESIS
PRESENTED
AS A REQUIREMENT
FOR THE MASTERS IN BIOCHEMISTRY

BY
DAMAN SINGH POKHREL

SEPTEMBER 2022

UNIVERSITÉ DU QUÉBEC À MONTRÉAL

CARACTERISATION PAR RESONANCE MAGNETIQUE NUCLEAIRE *IN VIVO* DE *AEROMONAS SALMONICIDA*, UNE BACTERIE PATHOGENE POUR LES SALMONIDES

MÉMOIRE
PRÉSENTÉ
COMME EXIGENCE PARTIELLE
POUR LA MAÎTRISE EN BIOCHIMIE

PAR
DAMAN SINGH POKHREL

SEPTEMBRE 2022

ACKNOWLEDGEMENT

Firstly, I would like to express my sincere gratitude to my supervisor, Prof. Isabelle Marcotte, for giving me a huge as well as challenging opportunity to pursue my master's degree in biochemistry at her reputed and esteemed laboratory with a scholarship. Without her tremendous support and guidance, this project would not have been completed smoothly. Prof. Isabelle Marcotte's motivation, expertise, knowledge, valuable advice, and suggestions throughout this project are the main reason behind the completion of my master's degree.

I also would like to thank my co-supervisor, Dr. Dror Warschawski, for his immense support and encouragement during this project. His amazing personality with profound wisdom and endless patience motivated me every day. His keen interest and broad vision in the project kept me inspired throughout the project. I really appreciated his support and guidance.

I would like to extend my sincere thanks to Dr. Alexandre Arnold for guiding me with his scientific expertise on NMR and his welcoming personality that enhanced my project for smooth completion. Moreover, his knowledge of NMR technology and his ideas helped me a lot for tackling the NMR issues during the project.

Moreover, I would especially like to acknowledge and extend my sincere thanks to Professor Steve Charette for providing me the bacterial strains and Professor David Dewez for granting me access to use his laboratory equipment on which part of the experiments were performed. They both not only participated in the evaluation of this manuscript, but also their valuable comments and suggestions helped me a lot to improve this manuscript before its final submission to UQAM.

I would like to thank David Giles and Steven Symes, from The University of Tennessee at Chattanooga, for helpful advice they gave us on the interpretation of FA incorporation by *A.s.s.*

I would also like to thank my lab family, especially, Alexandre Poulhazan, Kiran Kumar, Mathew Sebastiao, Florent Laydevant and Stéphane Beauclercq for helping me tirelessly for the past three years. I would also like to thank all my friends, teachers, Faculty members, and Professors who were always there for me when I needed help during my years in Montreal.

Moreover, I would like to thank UQAM's staff for providing me a family-like environment with selfless helping hands and the different associations involved with my project with financial and technical support. I would also like to acknowledge Natural Sciences and Engineering Research Council (NSERC), Canada, for providing the financial support to this project.

Lastly, I soulfully extend my gratitude to my parents, sister, and my beloved wife for believing in me. Without their love, care, motivation, and unconditional support, I would not have been able to accomplish my goals. Furthermore, your faith in me and your wishes are the source of inspiration for me.

TABLE OF CONTENTS

ACKNOWLEDGEMENT…… II
LIST OF FIGURES VI
LIST OF TABLES IX
LISTS OF ABBREVIATIONS, SYMBOLS AND ACRONYMS X
RÉSUMÉ XIII
ABSTRACT XV
CHAPTER I INTRODUCTION 1
1.1 FURUNCULOSIS 1
1.2 AEROMONAS SALMONICIDA 5
1.2.1 Virulent properties of *A.s.s* 6
1.2.2 Cellular organization of *Aeromonas salmonicida* 8
1.3 BACTERIAL CELL MEMBRANE 9
1.3.1 Phospholipids 10
1.2.2 Labeling strategy of bacterial membrane lipids 11
1.4 DEUTERIM SOLID-STATE NUCLEAR MAGNETIC RESONANCE (^{2}H SS-NMR) 15
1.5 OBJECTIVES 18
CHAPTER II DEUTERIUM LABELING AND CHARACTERIZATION OF *AEROMONAS SALMONICIDA* 20
2.1 EVOLUTION OF LABELING STRATEGY 20
2.2 MATERIALS AND METHODS 22
2.2.1 Materials 22
2.2.2 Purity test 22
2.2.3 Bacterial growth monitoring 23
2.2.4 Detergent optimization 23
2.2.5 Optimization of labeling strategy 24
2.2.6 Deuterium labeling 24

2.2.7 Level of deuteration 25
2.2.8 Cell viability assay 25
2.2.9 Lipid extraction 26
2.2.10 Phospholipid profile analysis by ^{31}P solution NMR 27
2.2.11 Fatty acids profile by GC-MS 28
2.3 *IN VIVO* ^{2}H SS-NMR AND M_2 ANALYSIS 28
2.3 MINIMUM INHIBITORY CONCENTRATION (MIC) AND MINIMUM BACTERICIDAL COMCENTRATION (MBC) 30
CHAPTER III RESULTS 32
3.1 OPTIMIZATION OF THE GROWTH TEMPERATURE 32
3.2 DETERMINATION OF THE LIPID PROFILE IN THE NATIVE STRAINS 34
3.3 OPTIMIZATION OF LABELING STRATEGY 39
3.3.1 Detergent selection 39
3.3.2 Optimization of the saturated-to-unsaturated FA chain molar ratio 41
3.3.3 Deuterium labeling of *A.S.S.* 44
3.4 *IN VIVO* ^{2}H SS-NMR AS A FUNCTION OF TEMPERATURE 47
3.5 CELL VIABILITY 48
3.5 MIC AND MBC ASSAY 49
CHAPTER IV DISCUSSION 50
4.1 ESTABLISHING THE ^{2}H-LABELING PROTOCOL 50
4.2 *IN VIVO* ^{2}H SS-NMR ANALYSIS AND CHANGE IN DYNAMICS 53
CONCLUSION AND PERSPECTIVES 56
APPENDIX A 58
APPENDIX B 61
APPENDIX C 63
APPENDIX D 66
BIBLIOGRAPHY 69

LIST OF FIGURES

Figure Page

1.1 Furunculosis symptoms of furuncle on the skins of salmons (Dallaire-Dufresne *et al.*, 2014), with permission 2

1.2 Scanning electron microscopy images of (A) wild type *A. salmonicida* (Meng *et al.*, 2017) with permission 5

1.3 Schematic representation of the Type III secretion system (T3SS) in Gram-negative bacteria (Hotinger et May, 2020) with permission 7

1.4 Diagrammatic representation of *A.S.S.* cell architecture 8

1.5 Structural representation of the cell wall composition of Gram-negative bacteria with lipopolysaccharides, peptidoglycan, lipoproteins lipids, etc. Adapted from Paracini *et al.*, 2022 (Paracini *et al.*, 2022) 9

1.6 Generalized structure of the bacterial phospholipid bilayer membrane with hydrophobic and hydrophilic regions 10

1.7 Structural representation of phospholipids: example of the phosphatidylethanolamine 10

1.8 Chemical structure of the dominant FAs chains present in *A.S.S.* lipids: palmitic acid (C16:0), palmitoleic acid (C16:1) and oleic acid (C18:1) 12

1.9 Schematic representation of deuterium labeling strategy and analysis of bacterial membranes 13

1.10 Schematic representation of the phospholipid synthesis from exogenous FAs bacteria 14

1.11 Comparison of static and MAS ^{2}H SS-NMR spectra and acquisition times for a bacteria sample (Warnet *et al.*, 2016) 18

2.1 Schematic representation of the methods used for the overall project 21

2.2 Schematic representation of the resazurin assay. The blue resazurin pigment is reduced to a pink resorufin pigment by the mitochondrial activity of living cells 25

2.3 Diagrammatic representation of MIC analysis of antibiotics by serial dilution (Ambaye *et al.,* 1997) 30

3.1 Brownish-red color pigment produced by pure (A) R3 and (B) R5 strains on FAM plates on the 7th day of incubation at 18°C 33

3.2 Growth temperature optimization of (A) R3 and (B) R5 strains at 18, 22 and 25^{o}C 33

3.3 (A)Wet and dry weight of the pellets of both R3 and R5 strains of *A.S.S.* at different growth phases, and (B) lipid extraction from the dried pellets 34

3.4 Representative ^{31}P solution NMR spectra of the different phospholipids extracted from (A) R3 and (B) R5 strains 35

3.5 Phospholipids proportions in (A) R3 and (B) R5 strains obtained from ^{31}P solution NMR spectra 36

3.6 GC-MS analysis of (A) the FAME mix, (B) R3 and (C) R5 fatty acid chain profile 37

3.7 Fatty acid profile of (A) R3 and (B) R5 strains as determined by GC-MS 38

3.8 Molecular structures dodecyl phosphocholine (DPC) and polyethylene glycol sorbitol monolaurate (Tween-20) 39

3.9 Determination of the detergent to be used for the micellization of the fatty acids. Growth curves of (A) R3 and (B) R5 were obtained at 18°C 40

3.10 Fatty acid profile obtained by GCMS for (A) R3 and (B) R5 strains grown in the presence of an equimolar ratio of OA and PA (0.1 mM) 41

3.11 Fatty acid profile determined by GCMS of (A) R3 and (B) R5 grown in the presence of exogenous FAs and harvested in the late-log phase 43

3.12 Fatty acid profile obtained by GCMS for (A) R3 and (B) R5 strains grown in the presence of an equimolar ratio of OA and PA-d_{31} (0.1 mM) 44

3.13 Fatty acid profile and deuteration level determined by GCMS of both *A.S.S.* strains grown in the presence of exogenous FAs and harvested in the late-log phase 45

3.14 MAS (10 kHz) ^{2}H SS- NMR spectra of (A) R3 and (B) R5 acquired at 8°C, 18°C and 28°C with 4096 scans for PA-d31 labeled R3 with 20 min of equilibrium time 46

3.15 Graphical representation of the M_2 of R3 and R5 acquired at 8°C, 18°C and 28°C with 4096 and 20 min of equilibrium time 47

3.16 Resazurin assay calibration curve for cell viability of R3 (A) and R5 (B) with different dilution of the control sample without before NMR 47

3.17 Cell viability of (A) R3 and (B) R5 at different time intervals before and after NMR (A = control; B = non-deuterated after washing; C = after 5 hours of NMR; D = after 11 hours of NMR) 48

3.18 MIC assay of polymyxin-B and Florfenicol against (A) R3 and (B) R5..... 49

3.19 MBC assay of (A) polymyxin-B and (B) florfenicol against (a) R3 and (b) R5. Visible growth observed on 0.5µg/mL and control. No growth observed on 1 µg/mL and 2 µg/mL for both antibiotics 49

LIST OF TABLES

Table Page

1.1 Table 1.1 Antibiotic resistance plasmids found in *A.s.s.* (Vincent *et al.*, 2021) 4

1.2 Table 1.2 Lipids headgroups identified in *Escherichia coli* (*E. coli*), *V. splendidus* and *B. subtilis* (PE - Phosphatidylethanolamine, PG - Phosphatidylglycerol and CL – Cardiolipin) 11

1.3 Fatty acid chains found in *A. salmonicida's* cell membrane (Bektas *et al.*, 2007; Morgan *et al.*, 1991) 12

3.1 ^{31}P Chemical shifts (ppm) of the phospholipids in *A.S.S.* R3 and R5 strains 35

3.2 Fatty acid analysis of the native strains by GC-MS 38

3.3 Fatty acid chain profile of R3 as determined by GC-MS analysis, with and without addition of exogenous FAs in the growth medium and harvested in the late-log phase 42

3.4 Fatty acid chain profile of R5 as determined by GC-MS analysis, with and without addition of exogenous FAs in the growth medium and harvested in the late-log phase 42

3.5 Level of deuteration analysis by GC-MS for both strains at the late-log phase 45

LISTS OF ABBREVIATION, SYMBOLS AND ACRONYMS

A.s.s.	*Aeromonas salmonicida* subspecies *salmonicida*
ACP	Acyl carrier protein
AMP	Antimicrobial peptides
CBB	Coomassie brilliant blue
$CDCl_3$	Deuterated chloroform
CL	Cardiolipin
CMC	Critical micelle concentration
CoA	Coenzyme A
D_1	Recycle delay
DPC	Dodecyl phosphocholine
EDTA	Ethylenediaminetetraacetic acid
FAs	Fatty acids
FAM	Furunculosis agar medium
FAME	Fatty acid methyl esters
GC-MS	Gas chromatography - mass spectrometry
HBSS	Hank's balanced salt solution
MAS	Magic angle spinning
M_2	Second spectral moment
OA	Oleic acid

OD	Optical density
PA	Palmitic acid
PA-d_{31}	Deuterated palmitic acid
PE	Phosphatidyl ethanolamine
PG	Phosphatidylglycerol
POA	Palmitoleic acid
Resazurin	7-hydroxy-3H-phenoxazin-3-one 10-oxide
SFA	Saturated fatty acid
SS-NMR	Solid state-nuclear magnetic resonance
S/N	Signal-to-noise
T3SS	Type III secretion system
Tween-20	Polyethylene glycol sorbitan monolaurate
UFA	Unsaturated fatty acids
TSB/TSA	Tryptic soy broth/Tryptic soy agar
v/v	volume/volume

RÉSUMÉ

Aeromonas salmonicida sous-espèce *salmonicida (A.s.s.)* est un agent pathogène responsable d'une maladie appelée « furonculose » chez les poissons, notamment les truites et les saumons. La présence d'une "couche A" et le développement de gènes de résistance aux antibiotiques rendent cette bactérie nuisible à l'aquaculture. La résonance magnétique nucléaire à l'état solide *in vivo* (RMN-ÉS) est un outil puissant et non invasif qui révèle la dynamique des phospholipides au niveau moléculaire, en sondant l'ordre de leurs chaînes acyles dans des bactéries intactes. L'objectif principal de ce projet était d'établir une stratégie de marquage au deutérium des membranes d'*A.s.s.*, et d'en réaliser une caractérisation biophysique par RMN-ÉS du ^{2}H *in vivo*. Nous avons utilisé deux souches d'*A.s.s.*, R3 et R5 respectivement avec et sans couche A. Nous avons optimisé la température de croissance, ainsi que le choix du détergent et des acides gras exogènes (AG) nécessaires au marquage. Le marquage avec 0,15 mM de Tween-20 et un rapport équimolaire de 0,1 mM d'acide palmitique deutéré (PA-d_{31}) et d'acide oléique (OA) a presque conservé le profil natif des AG saturés/insaturés, comme montré par GC/MS. La RMN du ^{31}P en solution n'a montré aucun changement dans le profil des têtes des lipides. Un niveau de deutération de presque 30 % de tous les AG a été atteint, suffisant pour fournir un rapport signal/bruit adéquat en RMN-ÉS du ^{2}H. Pour évaluer la réactivité des souches *A.s.s.* deutérées aux changements de dynamique des lipides, nous avons enregistré des spectres de RMN-ÉS en fonction de la température (8, 18 et 28° C). Les résultats ont montré que la membrane marquée était plus fluide lorsque la température augmentait. Ce projet présente la première deutération de membranes de *A.s.s.*, et jette les bases pour étudier le mécanisme d'action d'agents antimicrobiens dans des recherches futures.

Mots clés : résistance aux antibiotiques, RMN de l'état solide du ^{2}H *in vivo*, bactéries aquatiques, analyse des phospholipides, RMN du ^{31}P en solution.

ABSTRACT

Aeromonas salmonicida subspecies *salmonicida (A.s.s.)* is a pathogen responsible for a disease called “furunculosis” in fish, especially trouts and salmons. The presence of an “A-layer” and the development of antibiotic resistance genes make this bacterium harmful to aquaculture. *In vivo* solid-state nuclear magnetic resonance (SS-NMR) is a powerful and non-invasive tool that reveals the organization and dynamics of phospholipids at the molecular level, by probing the acyl chain ordering of lipids of intact bacteria in their natural environment. The main objective of this project was to establish a deuterium labeling strategy of *A.s.s.* phospholipid membranes and perform a biophysical characterization by *in vivo* ^{2}H SS-NMR. We used two *A.s.s.* strains, R3 and R5 respectively with and without an A-layer. We optimized the growth temperature, as well as the choice of detergent and exogenous fatty acids (FAs) required for labeling. Labeling with 0.15 mM of Tween-20 and an equimolar ratio of 0.1 mM of deuterated palmitic acid (PA-d31) and oleic acid (OA) almost conserved the native saturated/unsaturated FA profile, as shown by GC/MS. ^{31}P solution NMR showed no change in lipid head group profile before and after labeling. A deuteration level of almost 30% of all FAs was achieved, enough to provide an adequate signal-to-noise ratio in ^{2}H SS-NMR spectra. To assess the responsiveness of the deuterated *A.s.s.* strains for changes in lipid dynamics, we recorded *in vivo* ^{2}H SS-NMR spectra as a function of temperature (8, 18 and 28°C). Results showed the labeled membrane to be more fluid as the temperature was increased. This project presents the first deuteration of *A.s.s.* membranes and lays the foundation to study the mechanism of action of antimicrobial agents in future research.

Keywords: antibiotic resistance, *in vivo* ^{2}H SS-NMR, aquatic bacteria, phospholipid analysis, ^{31}P solution NM

CHAPTER I

INTRODUCTION

1.1 Furunculosis

Fish industry all over the world is suffering a huge loss due to various fish pathogens (Cipriano *et* Bullock, 2001). These opportunistic *bacteria* are the toughest challenge to all fish farmers to deal with due to their increasing susceptibility to infect fish in some conditions (decreased dissolved oxygen levels, increased environmental organic content, etc.) (Barton *et* Iwama, 1991). Furunculosis is one of the most dominant and systemic diseases with a high mortality rate in salmonids (salmon, trout, etc.) (Janda *et* Abbott, 2010). It is caused by *Aeromonas salmonicida* subspecies *salmonicida* (*A.s.s.*). From the past centuries, this bacterium is continuously causing huge losses to fish farmers as well as aquatic culture all over the world due to its virulence and also its capacity to resist antibiotic treatments (Dallaire-Dufresne *et al.*, 2014).

In Canada, specifically in Quebec, 30-60% of yearly fish infection are attributable to furunculosis outbreaks, causing huge losses in the fish farm industry (Cipriano et Bullock, 2001). This bacterium is responsible for numerous infections in important growth stages such as spawning and smolting fish as they are in immune-compromised stages of growth. The common symptoms of this disease in fish are furuncles (boils) in skins or muscles, sepsis, hemorrhages (skin, fin base, muscles, and internal organs), enlarged spleen, liver necrosis, etc., ultimately leading to fish death. There are different forms of furunculosis depending on the temperature, health, age, and so on (Bernoth, 1997). The chronic form is often characterized by the development of furuncles or boils

on the skin with other symptoms (lethargy, hemorrhages of fins, etc.) in older fishes (Figure 1.1). The acute form of infection is usually fatal for juvenile salmonids with few symptoms (necrosis, internal organs hemorrhages, etc.) or no evident clinical signs (Austin *et al.*, 2007).

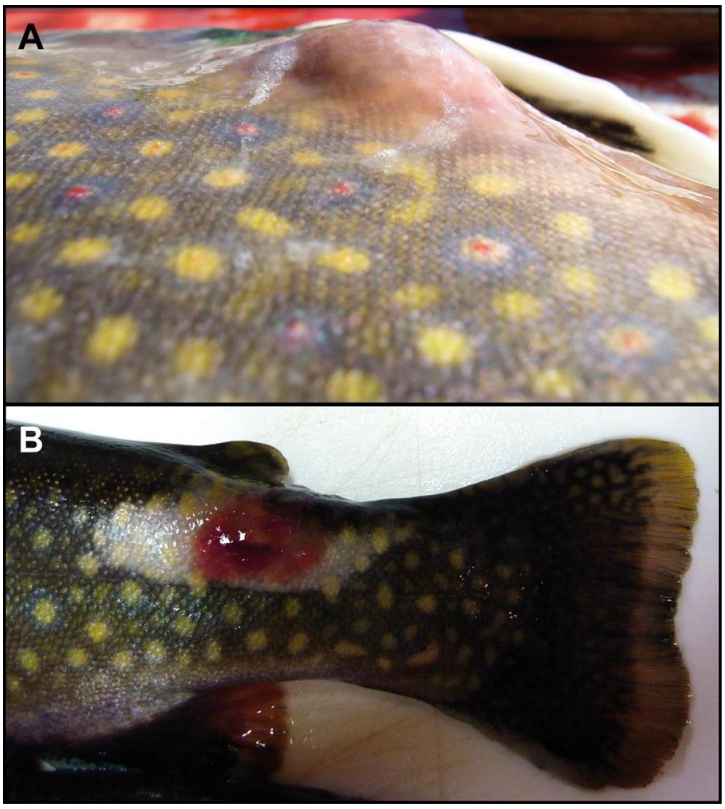

Figure 1.1 Furunculosis symptoms of furuncle on the skins of salmons (Dallaire-Dufresne *et al.*, 2014), with permission.

A.s.s. is a global threat, especially in the aquaculture of salmons and trout with high mortality rates due to furunculosis. *A.S.S.* is often resistant to the antibiotics, in Canada, approved by the Veterinary Drugs Directorate (VDD) to treat fish infections, such as oxytetracycline, florfenicol (a chloramphenicol analog), sulfamethazine or ormetoprim and sulfadiazine/trimethoprim (Trudel *et al.*, 2016) (Table 1). Florfenicol has become

the preferred choice of antibiotic because of its short withdrawal period (12 days) in contrast with other approved antibiotics (Marques *et al.*, 2018).

The phenomenon of antibiotic resistance by pathogens is usually due to excessive use of antibiotics, enabling such pathogens to develop multidrug resistance (Benveniste *et* Davies, 1973; Hasan *et* Al-Harmoosh, 2020). Bacterial resistance against antibiotics occurs in four principal forms (natural, acquired, cross-resistance and other multi-drug resistance). Natural resistance is usually due to its structural or intrinsic properties which prevent the antibiotics to reach the target (Antonoplis *et al.*, 2019). Acquired resistance occurs following alteration of chromosomal structure (plasmids, transposon, etc.) due to mutation (Andersson *et al.*, 2020). When a specific microorganism develops resistance to specific antibiotics, it is called cross-resistance (Etebu *et* Arikekpar, 2016). Multi-drug resistance is the most important type of the resistance shown by many bacteria especially *A.s.s.* (Dallaire-Dufresne *et al.*, 2014*)*. This type of resistance allows the bacterial species to protect themselves from antibiotics used against them (Alanis, 2005). This specific type of resistance is due to several resistance genes encoded in plasmids (R-plasmids) which confers resistance against several antibiotics (Nikaido, 2009).

The discoveries of drug resistance plasmids (R-factor) in *A.s.s* initiated from 1970s (Aoki *et al.*, 1971; Aoki *et al.*, 1972). R-plasmids such as pRAS1 (~45 kb) and pRAS2 (~48 kb) found to confer resistance against tetracycline, sulfonamide and streptomycin and pRAS3 (~12 kb) provide resistance to tetracycline (L'Abée-Lund *et* Sørum, 2000; Massicotte *et al.*, 2019; Sørum *et al.*, 2003). Similarly, pASOT (~47 kb), pASOT2 (~47 kb), and pASOT3 (~39 kb) plasmids were also later reported in *A.s.s* responsible for oxytetracycline resistance (Adams *et al.*, 1998). Similarly, other various multi- drug resistance plasmids are found which are mentioned in Table 1.1.

Table 1.1 Antibiotic resistance plasmids found in *A.s.s.* (Vincent *et al.*, 2021).

Plasmid	Length (kb)	Antibiotic resistance	References
pRAS1*, pRAS3.1 and pRAS3.2	45*, 12	Tetracycline Trimethoprim Sulfonamide	(Sandaa et Enger, 1994; Sørum et L'Abée-Lund, 2002)
pASOT3, (pASOT and pASOT2) *	39 47*	Oxytetracycline	(Adams *et al.*, 1998)
pAr-32	44	Chloramphenicol Streptomycin	(Sørum *et a*l., 2003)
pAsa4	167	Chloramphenicol Streptomycin Sulfonamide	(Dallaire-Dufresne et al., 2014; Reith *et al.*, 2008)
pAB5S9b	25	Tetracycline Florfenicol Streptomycin	(Vincent *et al.*, 2014)
pAsa8	110	Tetracycline Florfenicol Streptomycin Sulfonamide	(Trudel *et al.*, 2016)
pSN254b	152	Tetracycline Florfenicol Streptomycin Sulfonamide	(Vincent *et al.*, 2014)

Furunculosis can be easily transferred from a carrier fish to the others or through water contaminated by *A.s.s.* Vaccines were being developed against this ubiquitous disease from the 1970s (Fryer *et al.*, 1976; Midtlyng, 1997; Rodgers, 1990). By the 1990s, oil based adjuvants were used in vaccines for longer protection and increased fish

immunity against furunculosis (Fryer *et al.*, 1976). The first vaccine used against furunculosis infection was ASB (*A. salmonicida* bacterin), ASB-VAB-2 (*A. salmonicida- Vibrio anguillarum* bacterin) and ASB-ERB (*A. salmonicida- enteric redmouth* bacterin) (Midtlyng, 1997). However, they are very expensive, with most probable side effects, demanding for their inoculation and not always efficient (Midtlyng, 1997; Midtlyng, 2016). It is therefore important to understand this disease and its causative agents as a broader research perspective to develop therapeutic alternatives against furunculosis caused by this bacterium. Therefore, significant research is underway regarding antimicrobial peptides (AMPs), probiotics, or bacteriophages, to name a few (Bhat *et al.*, 2020; Hancock *et* Scott, 2000; Imbeault *et al.*, 2006).

1.2 *Aeromonas salmonicida*

Aeromonas salmonicida belongs to the order *Aeromonadales*, from the class of *Gammaproteobacteria* part of the *Aeromonadaceae* family within the genus *Aeromonas*. It was discovered by Emmerich and Weible in 1894 in a Bavarian brown trout hatchery. It is a Gram negative, motile/non-motile, non-spore forming rod-shaped bacterium ranging between 0.8 and 2.0 μm in size (Figure 1.2), scanning electron microscopy images of (A) wild type *A. salmonicida subspecies masouucida. A. salmonicida* comprises "typical" and "atypical" strains. Typical strains are usually isolated from salmonids and atypical strains are isolated from others (non-salmonid hosts) (Wiklund *et* Dalsgaard, 1998). These bacteria are further classified into five subspecies as *salmonicida, pectinolytica, achromogenes, smithia* and *masoucida* (Boone *et* Castenholz, 2001). Among these subspecies, *salmonicida* is mainly responsible for furunculosis which causes the death of salmons and other species, as previously mentioned. *A.s.s.* optimally grows at temperatures between 18 and 25 °C (Brenner *et al.*, 2005). However, it was reported a loss of some virulent genes occurs while growing this bacterium above 20 °C (Daher *et al.*, 2011; Ishiguro *et al.*, 1981).

A.s.s. is particular as it produces a brown water-soluble pigment that diffuses in agar in the presence of 0.1% tyrosine or phenylalanine.

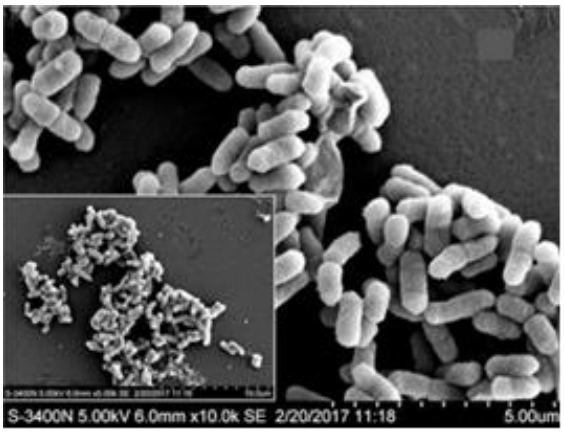

Figure 1.2 Scanning electron microscopy images of (A) wild type *A. salmonicida* subspecies *masoucida* (C4-wild type) (Meng *et al.*, 2017), with permission.

1.2.1 Virulent properties of *A.s.s.*

The virulence properties of *A.s.s* are due to different factors such as cell surface elements (pili, A-layer, lipopolysaccharide capsule, etc.,), extracellular toxins (cytolysin, serine protease, etc.,) and intracellular machinery (toxins secretion system, iron acquisition systems and quorum sensing system). Pili act as adherence support for *A.s.s* on the host cells (Boyd *et al.*, 2008). A-layer increases the hydrophobicity of the bacterial surface, resulting as a protection against macrophage cytotoxicity (Garduño *et al.*, 2000). Lipopolysaccharides mostly act as a permeability barrier against different molecules (toxins, detergents, antibiotics, etc.) for protecting the bacterial cell (Wang *et al.*, 2006). Extracellular toxins such as cytolysin or serine protease are responsible for lysis of host cells (Ellis *et al.*, 1988). *A.s.s.'s* virulent trait is due, among others, to the Type III secretion system (T3SS) (Dallaire-Dufresne *et al.*, 2014). T3SS is a complex system which comprises proteins responsible for the secretion and

translocation of effector proteins from the bacterial cytoplasm to the one of infected host cells (Lara-Tejero *et* Galán, 2019). As schematized in Figure 1.3, it consists of three parts: the basal body, the needle and the translocon. The basal body is attached to the bacterial membrane. It contains ATPase, which is responsible for the secretion of proteins. The needle acts as a sensor to detect the host cells and passage for the secreted proteins. The translocon mainly forms the pores in the host cells. These effector proteins can insert into the host cell, enabling them to enter the host cells through the pores (Cornelis *et* Van Gijsegem, 2000; Hotinger *et* May, 2020), as shown in Figure 1.3. The T3SS secretes effector proteins from the bacterium to the host cell leading to, among others, phagocytosis and apoptosis inhibition (Burr *et al.*, 2002; Frey *et* Origgi, 2016).

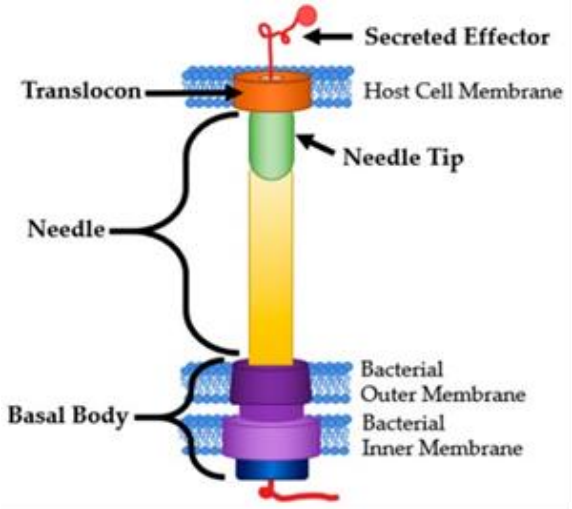

Figure 1.3 Schematic representation of the Type III secretion system (T3SS) in Gram-negative bacteria (Hotinger *et* May, 2020), with permission.

Moreover, extracellular molecules, such as enzymes (proteases, lipases, etc.) and other molecules are considered as other virulence factors. Mostly proteases secreted by this *A.S.S.* can hydrolyze the muscle proteins of the host cells thus leading to the appearance

of boils (Coleman *et* Whitby, 1993). Lipases combined with other genes also activate other enzymes for lipid hydrolysis of lipids of host cells (Lee *et* Ellis, 1990).

1.2.2 Cellular organization of *Aeromonas salmonicida*

Like other Gram-negative bacteria, *A.s.s.* is surrounded by four principal layers: the cytoplasmic lipid membrane, the cell wall (made of PGN), the outer lipid membrane, and the A-layer (made of glycoproteins) (Chu *et al.*, 1991; Huang *et al.*, 2008; Salton, 1953). The outer membrane is composed of phospholipids and lipopolysaccharides (LPS) covered with a unique array of proteins called the "A-layer" (Kay *et* Trust, 1991). The A-layer is composed of the protein VapA (50 kDa) which organizes as a tetragonal structure linked with diazoidosufanilic acid as schematized in Figure 1.4 (Kay *et al.*, 1981). As shown in Figure 1.4, the A-layer acts as a defense barrier against external molecules that induce resistance against specific immune defense and macrophage cytotoxicity. The A-layer proteins are encoded by the *vapA* gene (Gulla *et al.*, 2016).

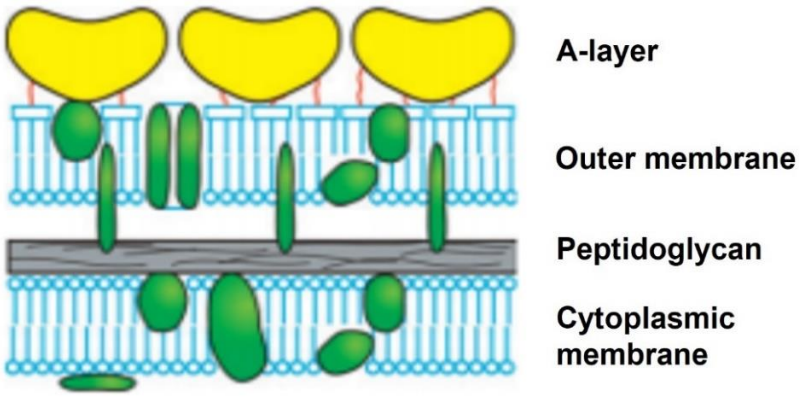

Figure 1.4 Diagrammatic representation of *A.S.S.* cell architecture (Sleytr *et al.*, 2014).

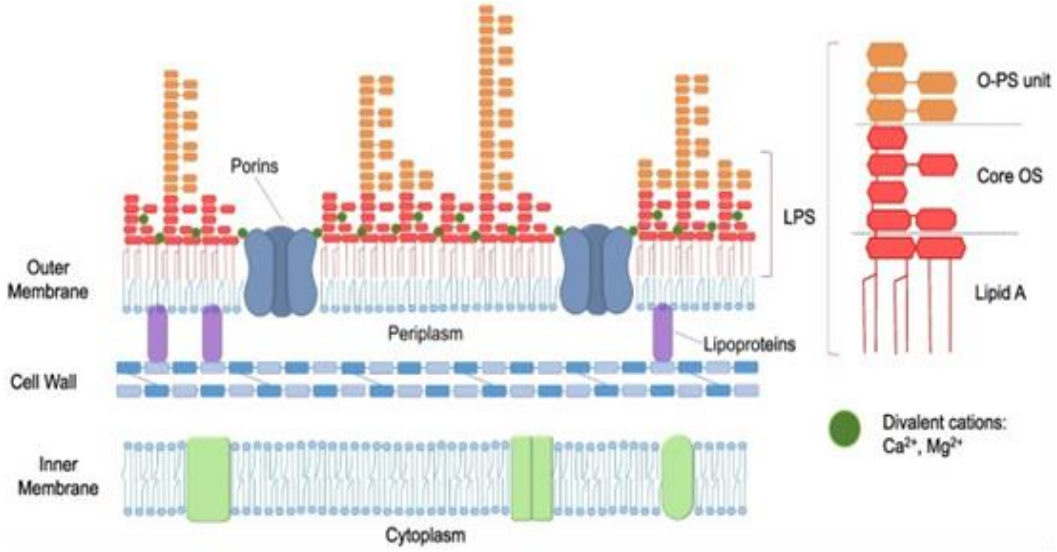

Figure 1.5 Structural representation of the cell wall composition of Gram-negative bacteria. Adapted from Paracini *et al.*, 2022 (Paracini *et al.*, 2022).

1.3 Bacterial cell membranes

Gram negative bacteria such as *A.s.s.* have a thin PGN (5-10 nm) as compared to Gram positive bacteria (30-100 nm) (Silhavy *et al.*, 2010). However, the plasma membrane of both bacterium types is rich in lipids and proteins. The phospholipids form a complex bilayer structure which notably regulates the molecular transport exchange between the cytosol and the external environment (Shan *et* Wang, 2015). The phospholipid bilayer presents a hydrophilic surface and a hydrophobic core (Figure 1.6) that helps the cell adopt a spherical shape in an aqueous medium. Phospholipids are thus an important protection barrier for the cell's organelles (Figure 1.4 and 1.5).

Lipopolysaccharides are made of the lipid A, a core oligosaccharide and an O-polysaccharide (O-antigen), as shown in Figure 1.5 (Munn *et al.*, 1982; Wang *et al.*, 2006). The PGN layer is very rigid and contributes to determine the shape of the cell wall. It is mostly composed N-acetyl glucosamine-N-acetyl muramic acids, which are

cross-linked by pentapeptide side chains disaccharide repetitive units (Figure 1.5) (Paracini *et al.*, 2022). Finally, the cytoplasmic membrane consists in a phospholipid bilayer made of phosphatidylethanolamine (PE), phosphatidylglycerol (PG) and cardiolipin (CL) (Warschawski *et al.*, 2011).

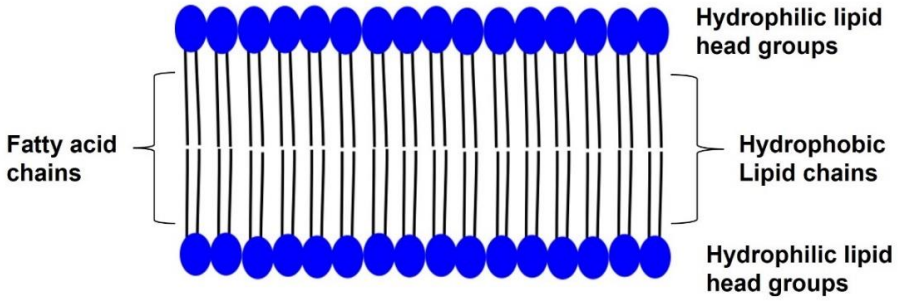

Figure 1.6 Generalized structure of the bacterial phospholipid bilayer membrane with hydrophobic and hydrophilic regions.

1.3.1 Phospholipids

Bacterial cell membrane's phospholipids are divided into three parts: the polar surface made by the phosphate group, the interfacial region comprising the glycerol portion, and the hydrophobic tails made by the fatty acid chains attached to the headgroup via ester linkages as shown in Figure 1.7 (Sohlenkamp *et* Geiger, 2016).

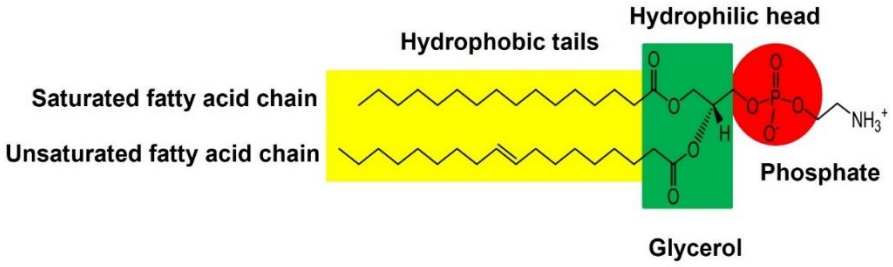

Figure 1.7 Structural representation of phospholipids: an example of the phosphatidylethanolamine.

Phospholipids are classified according to their headgroups. In bacterial cell membranes, the most dominant phospholipids are phosphatidylethanolamine (PE), phosphatidylglycerol (PG) and cardiolipin (CL), and their structures are displayed in Figure 1.8.

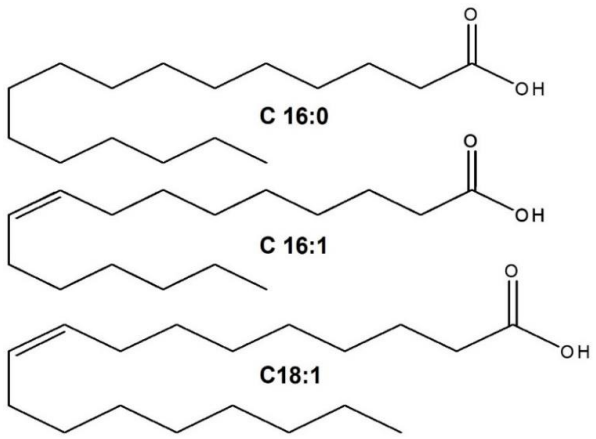

Figure 1.8 Chemical structure of the dominant FAs chains present in *A. salmonicida* lipids: palmitic acid (C16:0), palmitoleic acid (C16:1) and oleic acid (C18:1).

Phosphatidylethanolamine is dominant in most Gram negative bacteria (Bouhlel *et al.*, 2019). For example, *E. coli* contains about 75% of PE, 20 % of PG and less than 5% of CL. The marine bacterium *Vibrio splendidus* (*V. splendidus*) is made of 85% of PE, 10% of PG and 5% of CL (Bouhlel *et al.*, 2019). In contrast, *Bacillus subtilis* (*B. subtilis*) is dominated by PG (60 %), and contains 34 % of PE, and 6 % of CL according to previous studies summarized in Table 1.2 below (Laydevant *et al.*, 2022).

The lipid chains can be composed of saturated (SFA) or unsaturated (UFA) fatty acids (Figure 1.9). The bacterial membrane FA composition is often dominated by palmitic acid (PA) and oleic acid (OA) (Bouhlel *et al.*, 2019; Laydevant *et al.*, 2022). However, *A.s.s.* is dominated by palmitoleic acid (POA) and PA with 40-50% and 25-30% of overall FAs, respectively. The composition of *A.s.s.* is shown in Table 1.3.

Table 1.2 Lipids headgroups identified in *Escherichia coli* (*E. coli*), *V. splendidus* and *B. subtilis* (PE - Phosphatidylethanolamine, PG - Phosphatidylglycerol and CL – Cardiolipin).

Bacterial strains	Lipid head groups (%)			References
	PE	PG	CL	
E. coli	75	20	5	(Laydevant *et al.*, 2022)
B. subtilis	34	60	6	(Laydevant *et al.*, 2022)
V. splendidus	85	10	5	(Bouhlel *et al.*, 2019)

Table 1.3 Fatty acid chains found in *A. salmonicida's* cell membrane (Bektas *et al.*, 2007; Morgan *et al.*, 1991).

Fatty acids	Percentage (%)
C14:0	9
C16:0	24
C16:1	46
C18:1	8

1.3.2 Labeling strategy of bacterial membrane lipids

Professor Isabelle Marcotte's laboratory has established protocols for labeling lipid membranes with exogenous deuterated FAs for the study of not only bacterial membrane (*E. coli, B. subtilis* and *V. splendidus*), but also erythrocytes (Bouhlel *et al.*, 2019; Kumar *et al.*, 2022; Laadhari *et al.*, 2016; Tardy-Laporte *et al.*, 2013). Deuterium labeling was found to be efficient with 18% of Fas deuterated in *V. splendidus*, and

60% in *E. coli* (Bouhlel *et al.*, 2019; Laadhari *et al.*, 2016; Tardy-Laporte *et al.*, 2013). The incorporation of only deuterated palmitic acid (PA-d_{31}) resulted in some membrane perturbation by altering the SFA/UFA ratio (Warnet *et al.*, 2016). However, the ratio was nearly restored to that of the native strains by adding an equimolar ratio of OA and PA-d_{31}. Considering the low water solubility of Fas, the incorporation of Fas into the bacterial membrane requires the selection of a detergent to form mixed micelles, and the concentration of the detergent needs to be above its critical micelle concentration (CMC). Then a growth medium for the bacteria containing the micellized Fas is prepared, enabling the FA uptake and integration into different phospholipids as shown in Figure 1.9.

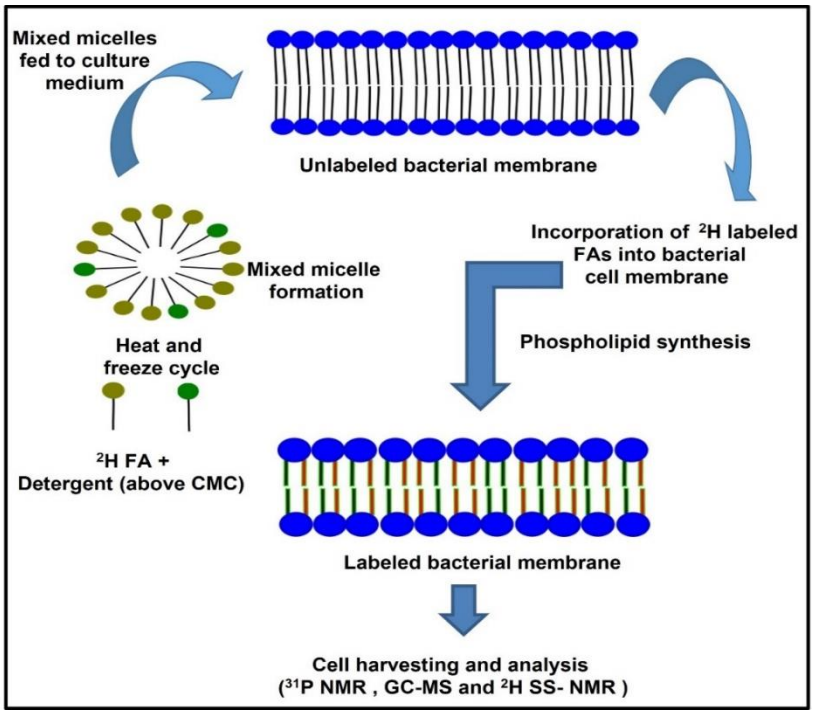

Figure 1.9 Schematic representation of deuterium labeling strategy and analysis of bacterial membranes.

The biochemical mechanism of the incorporation of exogenous FAs in the bacterial membrane phospholipid synthesis occurs via two mechanisms (Figure 1.10).

In the first mechanism, the exogenous FAs firstly bind with the *fadL* transport protein precursor in the outer membrane. They are transferred to acyl-CoA in the cytoplasm. Then FAs are linked to phosphatidic acid by the glycerol-3-phosphate acyltransferase. Acyl-CoA disintegration can also occur by β-oxidation (Zhang *et* Rock, 2008). In the second mechanism, the exogenous FAs are converted into PE by the acyl-carrier protein (ACP) and converted to phospholipids, as shown in Figure 1.10 (Byers *et* Gong, 2007). Our labeling protocol has been shown to incorporate fatty acyl chains exclusively in phospholipids, and not in lipopolysaccharides, hence it is mostly the plasma membrane that is labeled (Laadhari *et al*. 2016).

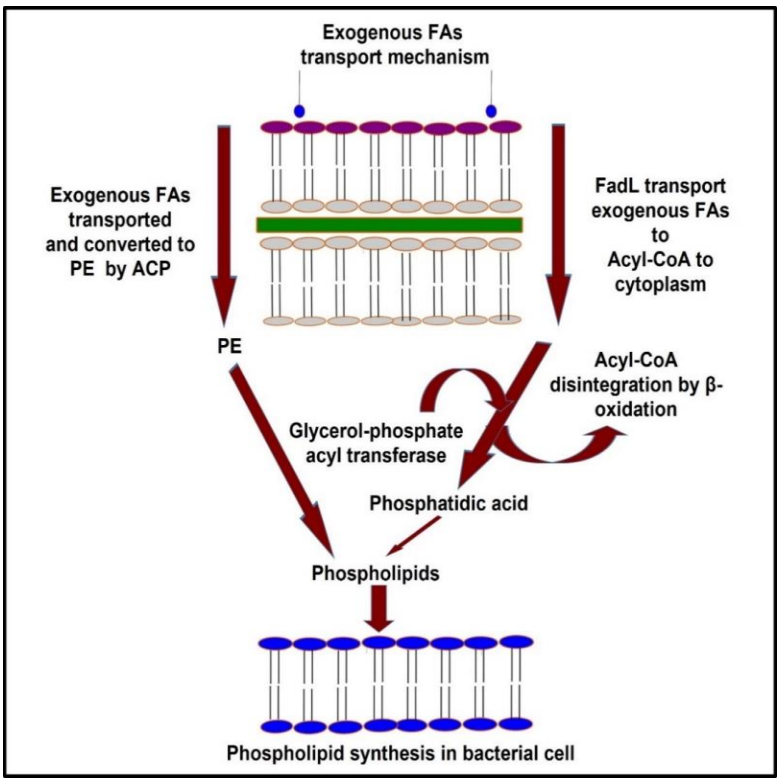

Figure 1.10 Schematic representation of the phospholipid synthesis from exogenous FAs in bacteria.

1.4 Deuterium solid state-nuclear magnetic resonance (^{2}H SS-NMR)

NMR is a non-invasive and powerful technique to probe the dynamics of proteins, lipids and other molecules involved in cellular integrity (Serber *et al.*, 2001). In the early 1970s, Oldfield *et al.* proposed static SS-NMR to study lipids, which became a breakthrough in biological NMR (Oldfield *et al.*, 1971; Oldfield *et al.*, 1972). However, the quality of the spectra obtained lacked sensitivity, but this was later addressed by the introduction of a 90° solid echo pulse (Stockton *et al.*, 1977). Although static SS-NMR experiments remain time-consuming and have less sensitivity, they provide valid information on the molecular order and dynamics of deuterated lipids in membranes.

Because the natural abundance of deuterium is 0.015%, isotopic enrichment is essential to enhance the signal. Moreover, a high level of deuterium incorporation is necessary to garner information of membrane dynamics and lipid acyl chains organization. Labeling membranes with deuterium is advantageous because it is a non-perturbating isotope (Davis, 1979; Seelig *et* Macdonald, 1987). SS-NMR is a non-invasive technique to study the biologically complex membranes, their structures, and dynamic properties such as membrane fluidity variations and structure. In the 1970s, ^{2}H NMR was dominantly focusing on model membranes (Seelig *et* Macdonald, 1987; Stockton *et al.*, 1977).

Membrane labeling in bacteria can be done by two different strategies. The first approach is to grow a mutant (auxotrophic) bacterial strain which is unable to synthesize or metabolize FAs, in the presence of labeled fatty acids and detergent micelles supplemented in the culture medium (Davis *et al.*, 1979; Pius *et al.*, 2012; Santisteban *et al.*, 2017). In 2013, Marcotte's laboratory showed that wild-type *E. coli* could be used for exogenous FA incorporation with detergent micelles in the culture medium (Tardy-Laporte *et al.*, 2013; Warnet *et al.*, 2016), therefore showing that auxotrophic bacterial strains were not needed. This strategy allows the bacterial strains to uptake exogenous deuterated PA and OA for the synthesis of deuterated

phospholipids in the cytoplasmic membrane, as shown in Figure 1.10. This work opened a new avenue for the *in vivo* dynamics characterization of bacterial membranes and facilitated the study of the interaction of different antibacterial compounds with labeled bacteria by *in vivo* ^{2}H SS-NMR.

Quadrupolar interaction is dominant in deuterium NMR, deuterium being a spin 1 nucleus, which leads to symmetric spectra with mirror peaks separated by the quadrupolar splitting ($\Delta\nu_Q$). The quadrupolar splitting depends upon two parameters: its orientation with respect to magnetic field, and the C-D bond location on the acyl chains. Phospholipids in liquid-crystalline membranes experience fast rotation along their longitudinal axis. To understand the C-D bond in a phospholipid bilayer with axial symmetry, the quadrupolar splitting can be calculated by equation 1.1 below,

$$\Delta\nu_Q(\delta) = \frac{3}{4}\frac{e^2qQ}{h}(3cos^2\theta - 1)S_{CD} \tag{1.1}$$

where (e^2qQ/h) is the static quadrupole coupling constant equal to 168 kHz for a C-D bond in acyl chains (Burnett *et* Muller, 1971), θ is the angle between the bilayer normal and the lipid long axis, S_{CD} is the mean square order parameter of deuterium bond vector.

When many deuterium nuclei are present, it is difficult to measure individual quadrupolar splittings. Spectral moment (M_n) measurement is an alternative to quantify the distribution of quadrupolar splittings in ^{2}H SS-NMR spectra, using the following equation 1.2 (Davis, 1979),

$$M_n = \frac{\int_0^\infty \omega^n f(\omega)d\omega}{\int_0^\infty f(\omega)d\omega} \tag{1.2}$$

where ω is the frequency and f(ω) describes the spectrum line shape.

^{2}H SS-NMR spectra recorded in the static mode are broad with low signal-to-noise (S/N) ratio. Such time-consuming experiments can be an obstacle to record *in vivo* data. Indeed, the perishable (microbes) samples could be destroyed. The use of magic-angle spinning (MAS) to record ^{2}H SS-NMR spectra proposed by Warnet *et al*. (Warnet *et al.*, 2016) has been an important milestones for *in vivo* experiments. MAS was described by Andrew *et.al.* in 1958, I.J. Lowe in 1959 and coined by C. J. Gorter in 1960 (Andrew *et al.*, 1958; Hennel et Klinowski, 2005; Lowe, 1959). Spinning the sample at an angle of 54.7° averages to zero the expression $(3cos^2\theta - 1)$ that is present in all anisotropic interactions (such as the quadrupolar interaction, see equation 1.1). The broad peak pattern is thereby reduced to a set of intense spinning sidebands centered around the isotropic frequency (Figure 1.11).

The ^{2}H labeling of lipid acyl chains combined to MAS is thus a significant tool to study the dynamics of biological membranes in living cells. Thanks to MAS, the sensitivity is increased, and therefore acquisition time is shortened, compared to ^{2}H SS-NMR spectra recorded in the static mode (Warnet *et al.*, 2016). The second spectral moment (M_2) allows quantifying changes in the membrane dynamics (Andrew, 1981; Davis, 1979; Maricq *et* Waugh, 1979), and can be calculated as in equation 1.3:

$$M_n = \omega_r^n \frac{\sum_{N=0}^{\infty} N^n A_N}{\sum_{N=0}^{\infty} A_N} = \frac{4\pi^2 \nu_Q^2}{5} < S_{CD}^2 > \quad (1.3)$$

ω_r is the angular spinning frequency, N is the number of side bands, and A_N is the area of each sideband measured by spectral integration.

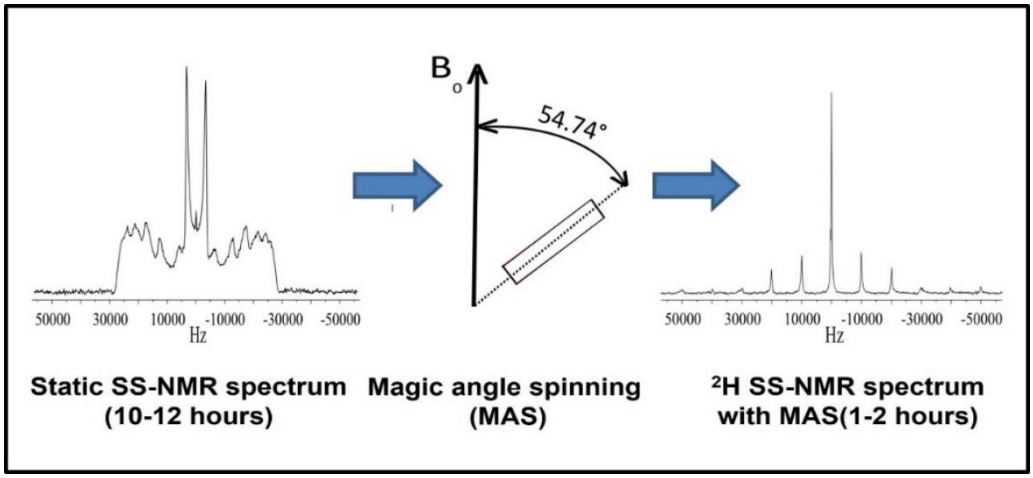

Figure 1.11 Comparison of static and MAS ^{2}H SS-NMR spectra and acquisition times for a bacteria sample (Warnet *et al.*, 2016).

1.5 Objectives

Our first hypothesis is that bacterial membrane dynamics and fluidity reflects the bacterial health. Our second hypothesis is that we can follow these dynamics by *in vivo* ^{2}H SS-NMR on bacterial with deuterated lipids. We will follow these dynamics when exposed to temperature variations or different antimicrobial agents as we have done in the past (Bouhlel *et al.*, 2019; Laadhari *et al.*, 2016). Bacteria have different pathways to incorporate exogenous FAs when added to the culture medium. When chosen appropriately, these exogenous FAs are ingested by bacteria and later converted into phospholipids and integrated in the membrane as shown in Figure 1.10. Therefore, the third hypothesis of this project is that *A.s.s.* will also allow us to label its membrane with exogenous deuterium labeled FAs, and then allow us to follow its health under various conditions by ^{2}H NMR.

The multidrug-resistant properties of *A.s.s.* are a major problem for the trout and salmon aquaculture sector in Canada, and the limited antibiotics used against this bacterium cannot be a long-term solution. It was already shown by different studies

that *A.s.s.* is continuously developing resistance to antibiotics (Trudel *et al.*, 2016). Therefore, other therapeutic alternatives might need to be envisioned. Antibiotics and most antimicrobials must pass through *A.s.s.* membranes to access different intracellular targets. Therefore, it is capital to study the interaction of antimicrobial agents with *A.s.s.* membranes. To do so, the membrane of *A.s.s.* must be characterized. It must also be labeled with stable isotopes to facilitate the specific study of the interaction of antimicrobial agents.

In this context, the first objective of this work was to characterize the cytoplasmic membrane of *A.s.s.* Then we successfully labeled the lipid bilayer with exogenous deuterated FAs, inspired by the previous labeling protocols of bacteria developed in Professor Isabelle Marcotte's laboratory. The labeling strategy and the results are discussed in the next chapters (Chapter II).

The second objective was to verify the integrity and test the response to changes in lipid dynamics that could eventually occur during peptide interaction. To do so, we monitored the change in dynamics as a function of temperature by *in vivo* ^{2}H SS-NMR. The results and methods are discussed in Chapter III.

CHAPTER II

DEUTERIUM LABELING AND CHARACTERIZATION *OF AEROMONAS SALMONICIDA* SUBSPECIES *SALMONICIDA*

2.1 Evolution of the labeling strategy

Our recent publications successfully demonstrated the efficient incorporation of exogenous FAs in *E. coli, B. subtilis,* and *V. splendidus* membranes for ^{2}H SS-NMR analysis, with significant S/N ratio of the spectra using MAS (Bouhlel *et al.*, 2019; Tardy-Laporte *et al.,* 2013; Warnet *et al.,* 2015; Warnet *et al.,* 2016). Based on the methodological approaches and results from the past years with these bacteria, the current project intends to propose the first protocol to ^{2}H-label the aquatic bacterium *A.s.s.* using FAs. For laboratory safety purposes, we used two mutant strains of *A.s.s.* that lack T3SS, M15879-11-R3 (with a-layer) and M15879-11-R5 (without A-layer) (Paquet *et al.,* 2019). Both strains were obtained by stressing them to grow at 25°C forcing them to rearrange the pAsa5 plasmid (Paquet *et al.,* 2019). We propose to label both mutant strains to compare the change of membrane dynamics with and without A-layer. This will enable us to understand the role of the A-layer, especially when antimicrobial agents interact with bacterial membranes.

First, the lipid head groups and FA composition of *A.S.S.* membranes were determined. The SFA/UFA molar ratio was of particular interest and guided the development of the protocol since the use of only SFAs can affect the dynamics of the lipid bilayer. Therefore, as previously done with *E. coli* and *B. subtilis* (Laydevant *et al.,* 2022), we

used both SFAs and UFAs in equimolar ratio in attempt to maintain the SFA/UFA molar ratio as close as possible to the native state.

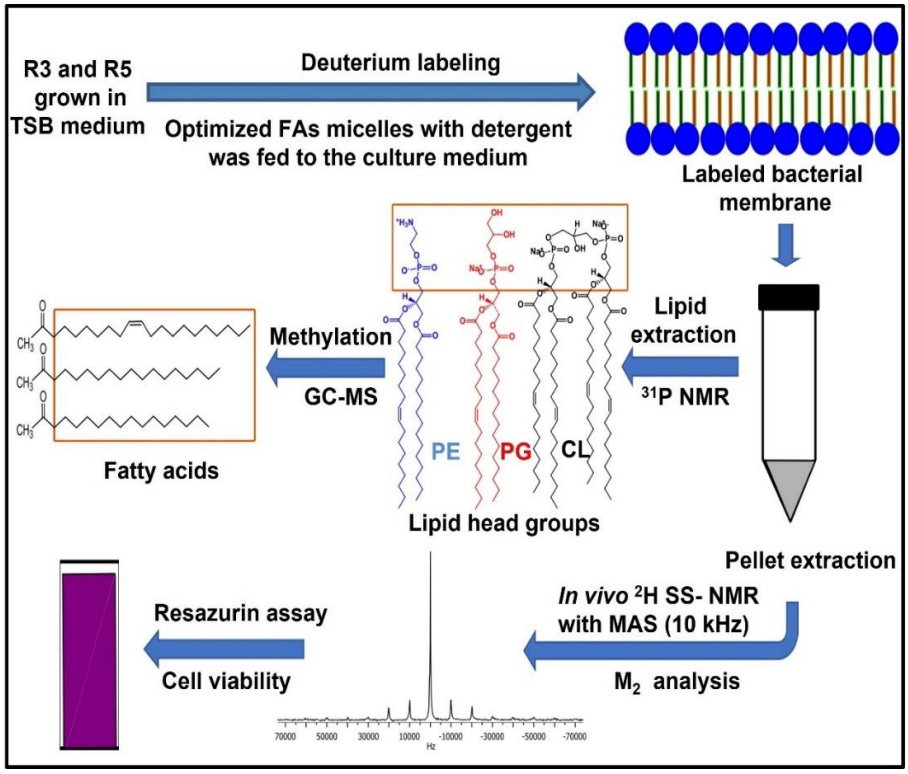

Figure 2.1 Schematic representation of the methods used for the overall project.

Since direct incorporation of exogenous FAs into bacterial cell membranes is not possible, solubilizing exogenous Fas with a detergent for the formation of mixed micelles was necessary. Therefore, the choice of a surfactant with a low CMC was optimized by growth curve monitoring and prevention of cell disruption. Following previous labeling protocols, we used dodecyl phosphocholine (DPC) and polyethylene glycol sorbitan monolaurate (Tween-20). We also used late-log growth phase to harvest the bacteria.

2.2 Material and Methods

2.2.1 Material

A.s.s. strains R3 and R5 were kindly provided by Professor Steve J. Charette from Université Laval (Québec, Canada) (Paquet *et al.*, 2019). Dodecyl phosphocholine (DPC) was purchased from Avanti Polar Lipids (Alabaster, AL, USA). Polyethylene glycol sorbitan monolaurate (Tween-20) was obtained from Bio Shop Canada Inc. (Burlington, ON, Canada). Palmitic acid, deuterated palmitic acid (PA-d_{31}), deuterated chloroform ($CDCl_3$), palmitoleic acid, oleic acid, deuterium-depleted water, fatty acid methyl ester (FAME) mix C4-C24 and 7-hydroxy-3H-phenoxazin-3-one 10-oxide (resazurin) were purchased from Sigma Aldrich (Oakville, Canada).

2.2.2 Purity test

A purity test for both strains was performed from the stock culture before the experiment. Furunculosis agar medium (FAM) was used for the detection of the pigmentation produced by the *A.s.s.* strains. This medium was prepared with bactotryptone, yeast extracts, tyrosine, sodium chloride and agar with nanopure water and the detailed quantities can be found in Appendix A (Griffin *et al.*, 1953). Using a sterile inoculation loop, a loopful of the sample was taken from the frozen stock culture for preculturing in 10-20 mL of tryptic soy broth (TSB) in a 50 mL sterilized flask. As detailed in Appendix 2, TSB contains tryptone, soy tone, dextrose, sodium chloride (NaCl) and dipotassium phosphate (K_2HPO_4) in nanopure water set to a pH of 7.3. The flask was incubated at 18 °C with a 200-rpm shaking for 48-72 hours. A loopful of culture was streaked on FAM Petri plates. The obtained pure culture was further tested for the presence and absence of A-layer with Coomassie brilliant blue (CBB) agar plate (Cipriano et Bertolini, 1988) (APPENDIX A). *A.s.s.* strains with A-layer absorb the CBB stain and form blue colonies whereas *A.s.s.* without A-layer form white colonies (Cipriano et Bertolini, 1988).

2.2.3 Bacterial growth monitoring

After confirming the strain purity, the tryptic soy agar (TSA) was prepared by adding right amount of agar in the TSB (Appendix A). The pure culture was streaked on tryptic soy agar plates for preculturing for further experiments. Preculturing was done as described in section 2.2.2. 1-2 mL of the preculture was added to 300 mL of sterilized TSB in a 1 L conical flask. Since the microplate reader was unfit to work below room temperature, the growth curve determination was done manually. Due to the slow growth process of *A.s.s.*, two sets of growth curves were run in parallel, with a 12 h shift, in the same incubator. Each set of experiments was run in triplicate. The first set was incubated at 9 A.M. (A set), and the second set at 9 P.M. (B set), on the same day. Therefore, the reading for 1-12 h, 24-36 h and 48-60 h was done with set A, while that of 12-24 h, 36-48 h and 60-72 h was done with set B. The spectrophotometer was set to a wavelength of 600 nm for optical density (OD) measurement. The OD of the aliquot (1 ml of the culture suspension) was determined at 0 h then monitored every 2 hours for each sample incubated at different temperatures (18^{o}C, 22 °C and 25 °C at 200 rpm shaking) until the values reached a plateau. At the end of the experiment, a growth curve was obtained by plotting the optical density at 600 nm (OD_{600}) as a function of time. All the experiments were done in triplicates and the results shown are the average in every set of experiments performed.

2.2.4 Detergent optimization

Protonated PA (0.1 mM) and the detergent (DPC or Tween-20) were mixed, then the strains were grown in the mixed micelles solution and the growth curve was monitored at 18^{o}C. The right amounts of protonated PA (7.7 mg) and either 55.2 mg of Tween-20 or 178.9 mg of DPC were dissolved in 10 mL of TSB. Both tubes were vortexed and heated at 95°C for 5-10 min to enable the dissolution of PA. The tubes were immediately transferred to liquid nitrogen for 5 min. This heat-freeze cycle was repeated 3-4 times until mixed micelles were obtained. After achieving a clear solution,

the temperature was stabilized to 50°C and the tubes were incubated for 5 min to make sure that PA was not precipitating. Since the R3 and R5 precultures reached an OD_{600} of around 1.7 after 72 hours, 15-17 mL of preculture was added to 273-275 mL of TSB, to reach an OD_{600} of 0.1 in the 290 mL of TSB in a 1 L flask. It was then incubated for 4 h before adding the 10 mL of mixed micelles. A 1 ml aliquot of the culture suspension was withdrawn from the flask at intervals of 2 hours and the OD_{600} was determined using a spectrophotometer. At the end of the experiment, the growth curve was obtained by plotting the OD_{600} values as a function of time (APPENDIX B).

2.2.5 Optimization of the labeling strategy

After determining the suitable detergent (0.15 mM of Tween-20 in 300 mL of TSB), we evaluated different exogenous Fas that naturally were present in both strains. More specifically, we individually tried 0.1 mM of PA, POA and OA, as well as different FA combinations, i.e., PA with OA as well as PA with POA, in an equimolar ratio of 0.1 mM. The mixed micelle preparation was made as above. However, the bacterial strain in TSB was maintained at an OD_{600} of 0.1 and incubated for 4 hours before adding the mixed micelles.

2.2.6 Deuterium labeling

After determining all the optimized conditions (growth temperature, detergent, and exogenous Fas) for labeling, we were finally able to achieve the labeling strategy for both strains of *As.s.* We used 0.1 mM of PA-d_{31} and 0.1 mM of OA micellized with 0.15 mM of Tween-20. The mixed micelles preparation with suitable detergent protocol was performed as above and the cell harvesting was done in the late-log phase.

2.2.7 Level of deuteration

Before going to ^{2}H SS-NMR experiments for verifying the change in dynamics of the lipid bilayer as a function of temperature, it was important to know the level of deuteration of the FA chains. The higher the level of deuteration, the higher the S/N

ratio for verifying the dynamics from the acquired ^{2}H SS-NMR spectra. The level of deuteration was assessed by GC-MS analysis as below (Section 2.2.11).

2.2.8 Cell viability assay

A resazurin assay was performed to determine the proportion of viable cells before and after NMR experiments. In this assay, live cell's mitochondrial respiratory chain mechanism reacts with the non-fluorescent blue resazurin, and the reduction of the dye will lead to a red fluorescent resorufin pigment as shown in Figure 2.2 (Riss *et al.*, 2016).

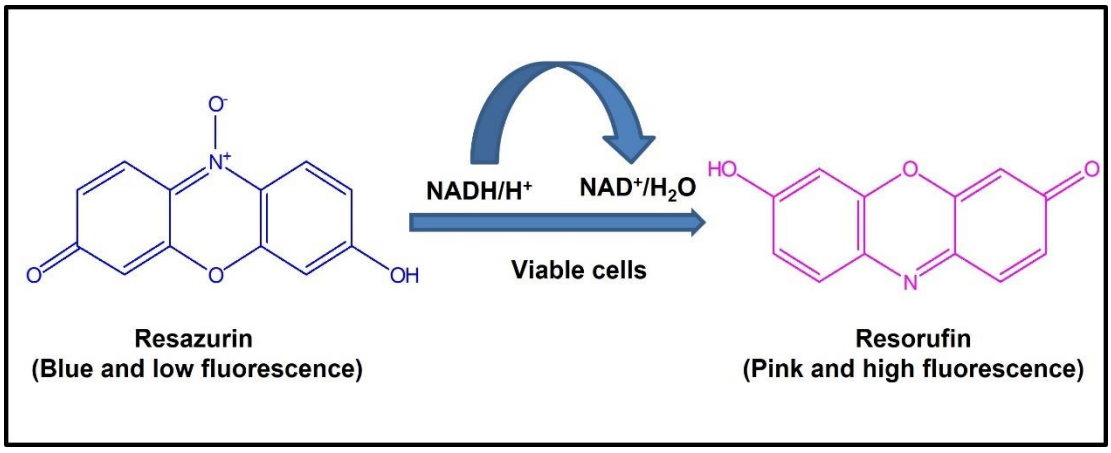

Figure 2.2 Schematic representation of the resazurin assay. The blue dye resazurin pigment is reduced to a pink resorufin pigment by the mitochondrial activity of living cells (Riss *et al.*, 2016).

Samples were diluted to an OD_{600} of 0.1 and the calibration curve of the viable cells (100%, 75%, 50% and 25%) was obtained by plotting the OD600 as a function of time. The 500 µM resazurin was prepared in a sterile Hank's balanced salt solution (HBSS) where 6.28 mg of resazurin was mixed with 50 mL of HBSS. The 500 mL of 500 µM stock solution was prepared and stored at 4°C. Cells before and after the NMR experiment were diluted to an OD_{600} of 0.1. In 96-well plates, the blank was taken as

10 µL resazurin + 90 µL buffer. The positive control sample (100% reference) was taken as 100 µL (cells + buffer). A total of 90 µL of the cells were added to the different wells and 10 µL of resazurin were also added in the same well so that each well contained a 50 µM resazurin concentration for 100 µL of every well. The fluorescence was recorded using a 520 nm excitation / 590 nm emission filter set for an hour. The cell viability was calculated after one hour using equation 2.1:

$$\text{Cell viability (\%)} = \frac{Sample - mean of blank}{Control - mean of blank} \times 100\% \quad (2.1)$$

2.2.9 Lipid extraction

Both strains were grown in TSB and incubated at 18°C with a 200-rpm shaking. The mid-log phase was observed after 36 hours with and an OD_{600} of 0.8, while the late-log phase occurred after 48 hours and an OD_{600} of 1.7 for R3 and 1.4 for R5. Pellets were collected and centrifuged at 3400 rpm for 10 min at 4°C, then washed with 0.88% NaCl in nanopure water and again centrifuged at 3400 rpm for 10 min at 4°C. The supernatant was discarded. The weight of wet and dry (lyophilized) pellet was determined and was typically between 50-100 mg for dry pellets. The freshly harvested pellets were used for cell viability assays, as well as phospholipid head groups and FAs profile analysis.

The polar lipid extraction protocol consists in a slight modification of Folch H_2O technique (Folch *et al.*, 1957). The dry pellets were mixed with 25 mL dichloromethane: methanol (2:1, v/v) and sonicated thrice at 8W on an ice bath for 1 min each time. The sample was transferred to a separating funnel and the volume was made to 50 mL by adding 25 mL of the $CHCl_2$:CH_3OH solution. A total of 13.5 mL of 0.88% KCl solution was added to the mixture and mixed by shaking and degassing. The organic phase (bottom of the separating funnel) was collected and dried under a

nitrogen flow at 40°C. The lipids were then collected, lyophilized and the weight determined (2-5 mg, typically).

2.2.10 Phospholipid profile analysis by ^{31}P solution NMR

^{31}P solution NMR experiments are reliable for the determination of the lipid profile (Laydevant *et al.*, 2022). The chemical shift values of different headgroups such as PE, PG or CL are well known and enable peak assignment in the ^{31}P NMR spectra, thus allowing monitoring potential changes in the lipid headgroup profile of both strains. The ^{31}P NMR analysis was done after the polar lipid extraction and before the methylation step. The lyophilized lipids were mixed with 500 µL of $CDCl_3$, 200 µL of CH_3OH and 50 µL of an ethylenediaminetetraacetic acid (EDTA) aqueous solution at pH 6.0 (Estrada *et al.*, 2008). The mixture was vortexed and transferred to NMR tubes. The tubes were sealed (APPENDIX C).

The ^{31}P solution NMR analysis was performed with a 600 MHz AVANCE III-HD NMR spectrometer (Bruker, Milton, ON, Canada). The spectrometer was equipped with a 4 mm probe operating at 242.84 MHz for ^{31}P detection. Spectra was acquired at 25°C using a 90° pulse of 15 µs using proton (^{1}H) decoupling. The acquisition was obtained with 128 scans and a recycle delay (D1) of 10 s for a total of 22 min, with a spectral width of 50 ppm and 8K data points. All the peaks were integrated to deduce the proportions of the different phospholipids. Since CL contains two ^{31}P atoms, the integral was divided by two.

2.2.11 Fatty acid profile analysis by GC-MS

The lipids from the ^{31}P solution NMR tubes were collected in a vial and the EDTA layer was carefully separated with a Pasteur pipette. The collected lipids were dried under a nitrogen flow at 40°C. The sample was then subjected to hydrolysis and methylation using 2 mL of H_2SO_4 (2% in MeOH) and 0.8 mL of toluene for 10 min at 100°C. The phase separation was done, and the upper layer of the tube was collected

in a separate vial. The content of the vial was dried under an N_2 flow at 40°C. GC-MS analysis, the final extracts were diluted in a hexane solution and adjusted to a volume of 0.5 mL. A commercial fatty acid methyl ester (FAME) mix (C4-C24) was prepared as the standard for parallel FAs analysis by GC-MS for verifying any change in FA profile between both strains of native *As.s.* as well as bacteria grown under addition of exogenous FAs, deuterated or not (APPENDIX C).

GC-MS analyses were performed using an Agilent Technologies 7890 A GC/ 5975C MS system equipped with electron ionization (70 eV). A total of 1 µL of the sample was injected to the silica capillary of 30 m × 250 µm × 0.25 µm of a HP-5MS (Santa Clara, CA, USA) with a split mode of 50:1. The holding temperature of the column was maintained to 140°C for 5 min followed by an increase to 300°C at the rate of 4°C/min. The helium flow was maintained constant at 0.5205 mL/min. A full scan mode was used on an m/z interval of 40-600. The total chromatogram covered approximately 40 min. Peaks were identified by comparing the retention times and m/z values with the standard FAME mix peaks. The integration of the area under each peak was used to calculate the percentage of each FA by comparing with the standard FAME mix. This GCMS analysis also allowed determining the level of deuteration in the deuterated bacteria samples.

2.3 *In vivo* ^{2}H SS-NMR and M_2 analysis

Both labeled bacterial strains were grown in a TSB medium (300 mL) in a 1L flask. The bacteria pellet was harvested in the late-log phase after 48-52 hours of culture. About 5-6 washing cycles were done using 0.88% NaCl in nanopure water and centrifuged at 1500 g. A final rinsing step was done with deuterium-depleted water with 0.88% of NaCl and again centrifuged at 1500 g. The pellet was collected and transferred to an NMR rotor (4-mm ZnO_2 rotor). The wet pellet was approximately of 100 mg when the rotor was fully filled. The rotor was inserted into the NMR probe.

Every set of experiments was done at three temperatures (8, 18 and 28°C). All ^{2}H SS-NMR experiments were carried out using a Bruker Avance III HD Wide Bore 600 MHz NMR spectrometer (Milton, ON, Canada) and a double-resonance magic angle spinning (MAS) probe tuned to 92.1 MHz. Samples were spun at 10 kHz and the spectra were recorded using a rotor-synchronized Hahn echo with 4 μs 90° pulses (8 μs 180°) separated by an echo delay of 96 μs, a recycle time of 1 s, using 4096 scans, a spectral width of 1 MHz and an acquisition time of 50 ms. The total experimental time per sample was approximately of 1 hour. Spectra were zero-filled to 64 k points and processed with an exponential line broadening of 100 Hz prior to Fourier transform. The spectrum processing was initially done with Bruker's Topspin software for spectral acquisition at 10 kHz after pulse calibration with 100 Hz of line broadening. The number suppressed point (nsp) was set between 4-10 from the spectrum with flat baseline and easy phasing.

The M_2 analysis was done with MestreNova software V12.0. Using the manual threshold option in the software, the zone was picked for peak-picking and peaks were refined by removing the unwanted peaks. For analysis, the new fit region was picked by picking the zone for fitting after eliminating the unwanted peaks (H_20 peak and others). With the selected new fit region, a new spectrum was created. The whole spectrum was integrated at once with the script 'MomentsSpectraux.qs'.

2.4 Minimum inhibitory concentration (MIC) and minimum bactericidal concentration (MBC)

MIC is the lowest concentration of any antimicrobial compounds that completely inhibits the growth of microorganism (Kowalska-Krochmal *et* Dudek-Wicher, 2021; Wiegand *et al.*, 2008). MBC is the minimum concentration of any antimicrobial agent that can completely kills the microorganism (Rodríguez-Melcón *et al.*, 2021). They are generally expressed in μg/mL.

We used serial dilution to determine the MIC for two antibiotics (Polymyxin-B and Florfenicol) (Ambaye *et al.*, 1997). Different concentrations of the antibiotics ranging from 0.032 to 32 µg/mL were prepared. 1 mL of TSB was added to each well of a 12 well-plate. 1 mL of 32 µg/mL of antibiotics was added to the first well and mixed thoroughly. 1ml from the first well of mixed media and antibiotics was transferred to the second well (16 ug/mL) and we repeated this dilution until the 11th well as shown in Figure 2.3. The final 1 mL from the 11th well is discarded. 20 µl of the bacterial suspension of Mc Farland standard of 0.5 was added to all the wells, except the first one (blank), and no antibiotics was added to the 12th well. The plate was incubated at 18°C for 72 hours and OD was measured at 600 nm, taking the first well as a reference. Determination of the MIC was done by plotting the OD *vs* the concentration of antibiotics used.

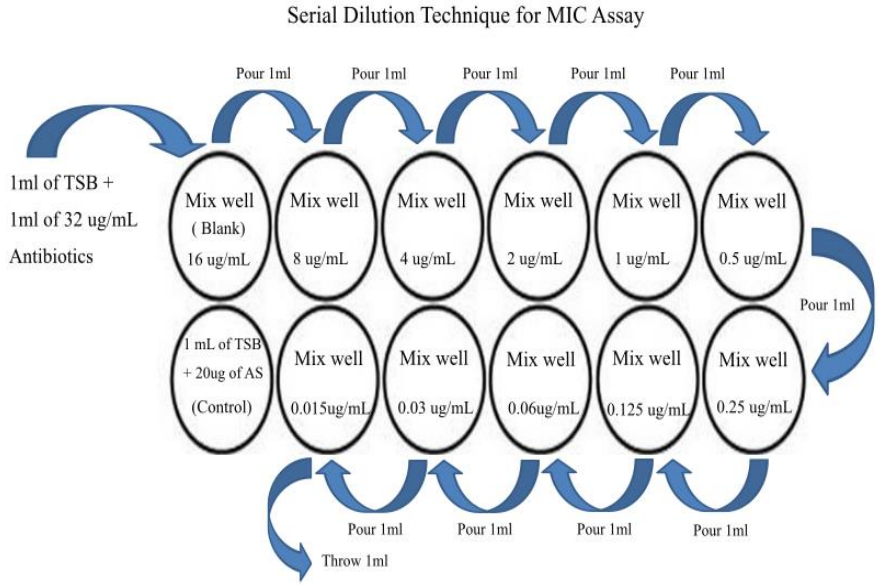

Figure 2.3 Diagrammatic representation of MIC analysis of antibiotics by serial dilution (Ambaye *et al.*, 1997).

MBC was determined by taking two samples above the MIC and one sample below the MIC from the above well plates. TSA plates are partitioned into four parts: a positive control without antibiotics, and three parts with samples above and below MIC. An inoculum of each sample was inoculated with the sterile inoculation loop in the TSA plates and the plates were sealed. The TSA plates were incubated at 18°C for 72 hours. The MBC is determined by examining the plates after incubation.

CHAPTER III

RESULTS

3.1 Optimization of the growth temperature

The first step prior to the labeling of a bacterium is to optimize the growth temperature. Depending on the particular strain, *Aeromonas salmonicida* grows at temperatures between 18 and 25 °C. It produces a particular brown water-soluble pigment in the presence of 0.1% tyrosine or phenylalanine that diffuses in agar as shown in Figure 3.1. Before optimizing the growth temperature of both *A.s.s.* strains, a purity test was conducted in furunculosis agar. The pigmentation was slightly visible after 3 days of incubation but was clearly visible after 6 days for both strains, confirming the purity (Figure 3.1). R3 colonies were darker than R5 colonies (Appendix D). The obtained pure culture was further tested for the presence and absence of A-layer with Coomassie brilliant blue (CBB) agar plate. CBB plates showed that the strain with A-layer (R3) absorbed the brilliant blue colorant pigment, while R5 remained non-pigmented (Paquet *et al.*, 2019) (APPENDIX D). Both strains of *A.s.s.* were grown at 18, 22 and 25^{o}C. As shown in Figure 3.2, the optimum growth temperature was found to be 18°C. It takes 40-45 hours to reach mid-log phase and 68-80 hours to reach the late-log phase. In addition, we observed that growth of both strains was slowed down when increasing

the temperature. Therefore, a temperature of 18ºC was used to perform the characterization of both strains for labeling.

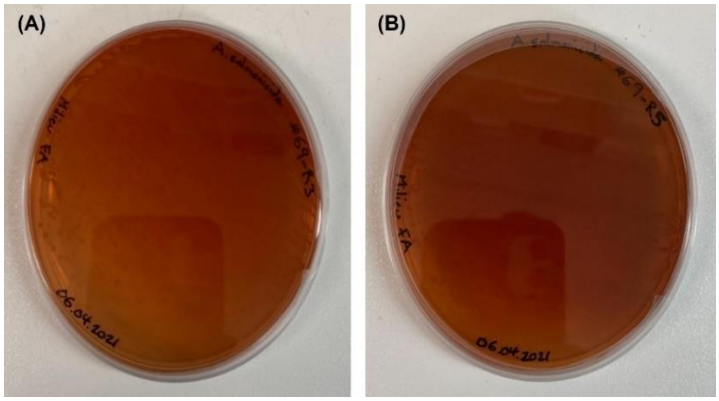

Figure 3.1 Brownish-red color pigment produced by pure (A) R3 and (B) R5 strains on FAM plates on the 7th day of incubation at 18°C.

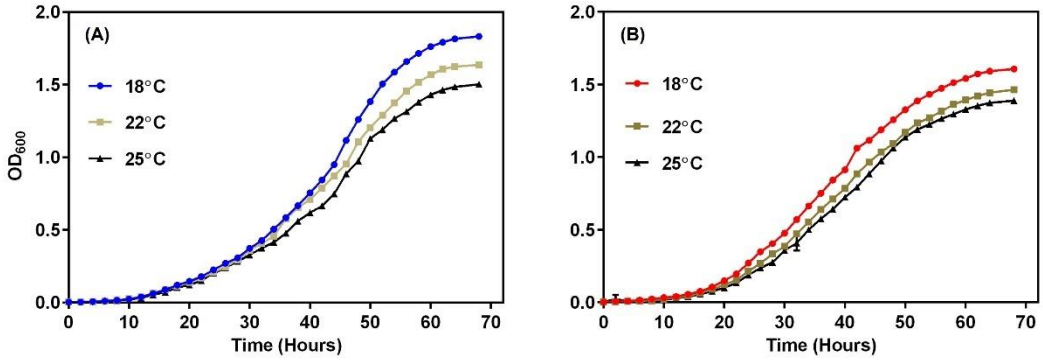

Figure 3.2 Growth temperature optimization of (A) R3 and (B) R5 strains at 18, 22 and 25ºC.

3.2 Determination of the lipid profile in the native strains

Before optimizing the deuteration protocol of the bacteria, the lipid content had to be determined. To do so, both strains were grown in 300 mL of TSB, in 1000 mL flasks

at 18°C, and were harvested at mid-log and in the late-log phases. The OD of the late-log phase for R3 and R5 was observed approximately of 1.8 and 1.6, respectively before the pellet harvesting as shown in Figure 3.2. The pellets were distinctive from each other. Plain surface on the top was observed on R5 pellets whereas rough surface was observed on the top of the pellet after centrifugation (APPENDIX D). The weight of the wet pellets was found to be 250-300 mg at mid-log and 500-550 mg in the late-log phase, for 300 mL of initial culture volume, as shown in Figure 3.3 A. When lyophilized, the pellets weight was found to be 45-55 mg and 95-105 mg for the mid-log and late-log phases, respectively (Figure 3.3 A). The lipid extraction was done on the dry pellets using Folch's protocol (Folch *et al.*, 1957). At the mid-log phase, the amount of dry lipids was found to be of 2-2.5 mg for 40-50 mg of dry pellets for both strains, representing about 6% of the dry weight (Figure 3.3 B). However, when harvested at the late-log phase, the amount of lipid extracted from both strains were found to be 4-4.5 mg for 50-60 mg of dry pellets, i.e., about 8% of the dry weight (Figures 3.3 B).

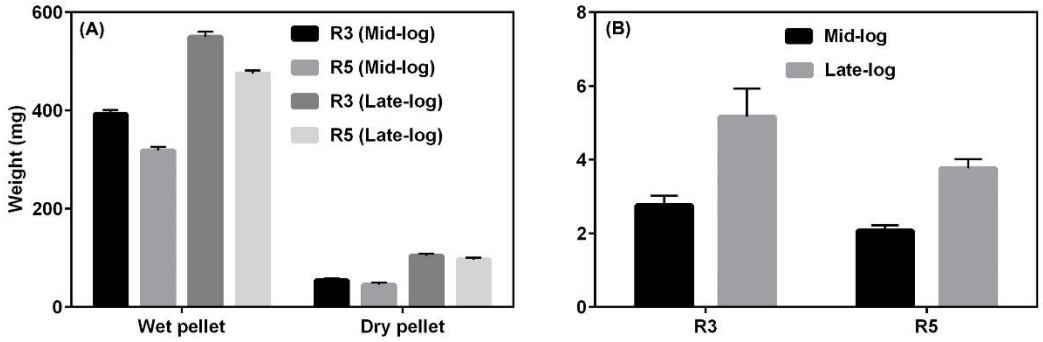

Figure 3.3 (A) Wet and dry weight of the pellets of both R3 and R5 strains of *A.s.s.* at different growth phases in 300 mL of initial culture volume, and (B) lipid extraction from the dried pellets.

Due to the 100% natural abundance of phosphorous-31 and its high gyromagnetic ratio (10.84×10^7 rad T^{-1} s^{-1}), ^{31}P solution NMR can easily detect the phosphorous atom in the phospholipids headgroup, as shown in Figure 3.4 A, B. ^{31}P chemical shifts of the phospholipids headgroups (PE, PG and CL) displayed in Table 3.1 are constant for both strains of bacteria in both growth phases. The chemical shift values of compare well with Laydevant et al. who found 0.65 for PG, 0.07 for PE and 0.40 for CL in the Gram-negative *E. coli.* (Laydevant *et al.*, 2022).

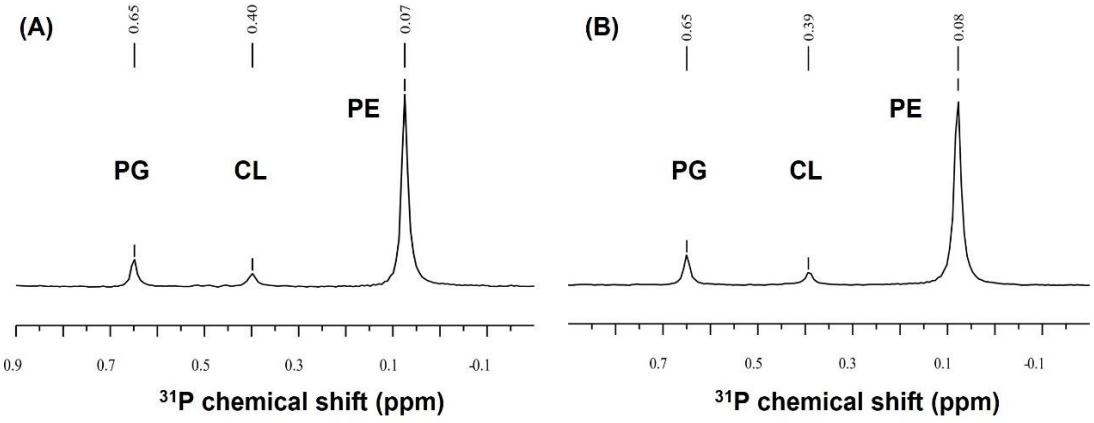

Figure 3.4 Representative ^{31}P solution NMR spectra of the different phospholipids extracted from (A) R3 and (B) R5 strains (PE - Phosphatidylethanolamine, PG - Phosphatidylglycerol and CL – Cardiolipin).

Table 3.1: ^{31}P Chemical shifts (ppm) of the phospholipids in *A.s.s.* R3 and R5 strains (PE - Phosphatidylethanolamine, PG - Phosphatidylglycerol and CL – Cardiolipin).

Strain	PG	CL	PE
R3	0.65	0.40	0.07
R5	0.65	0.39	0.08
B. subtilis	0.65	0.40	0.07

The ^{31}P solution NMR spectra were used to determine the proportions of phospholipids present in both strains. To do so, all peaks were integrated. The results in Figure 3.5 (A and B) showed that at the mid-log stage, CL represents approximately 2% of the phospholipids. However, this proportion is doubled at the late-log phase. PE is the dominant lipid (78-80%) followed by PG (12-15%) in both strains. These results are similar to Bouhlel *et al*. and Laydevant et al., who also found a similar trend and lipid profiles in *V. splendidus* and *E. coli* at mid-log and late-log phase as shown in Figure 3.5 and Table 3.1 (Bouhlel *et al.*, 2019; Laydevant *et al.*, 2022).

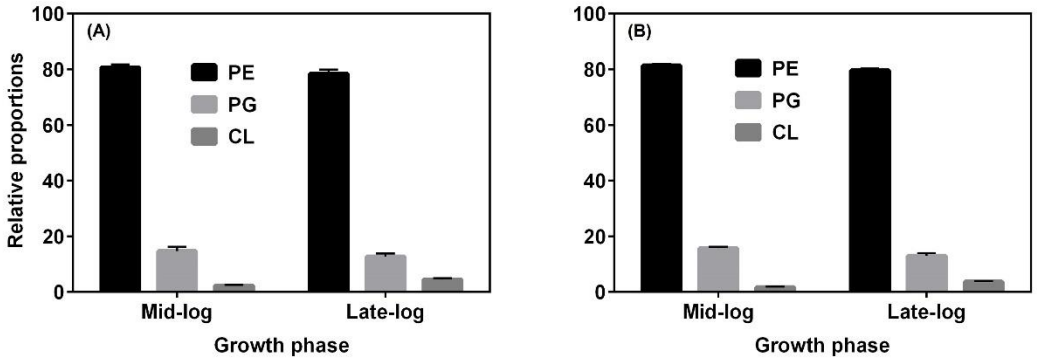

Figure 3.5 Relative phospholipid proportions in (A) R3 and (B) R5 strains obtained from ^{31}P solution NMR spectra.

The FA chain profile in R3 and R5 strains without labeling was verified and referenced with respect to a FAME C2-C24 mix. Overall, 27 peaks were verified using the retention times as shown in Figure 3.6 and Table 3.2. There are four abundant FAs present in both strains. More specifically, the GC-MS analysis shows that the FA composition of the cell membrane is mostly dominated by C16:1 (45-50%), C16:0 (25-30%) and C18:1 (15-20%), as shown in Table 3.2 and Figure 3.8. The SFA/UFA ratio of native R3 and R5 at mid- and late-log growth phases was constant, around 0.5. This value is important as it should be kept constant when the bacterial will be labeled.

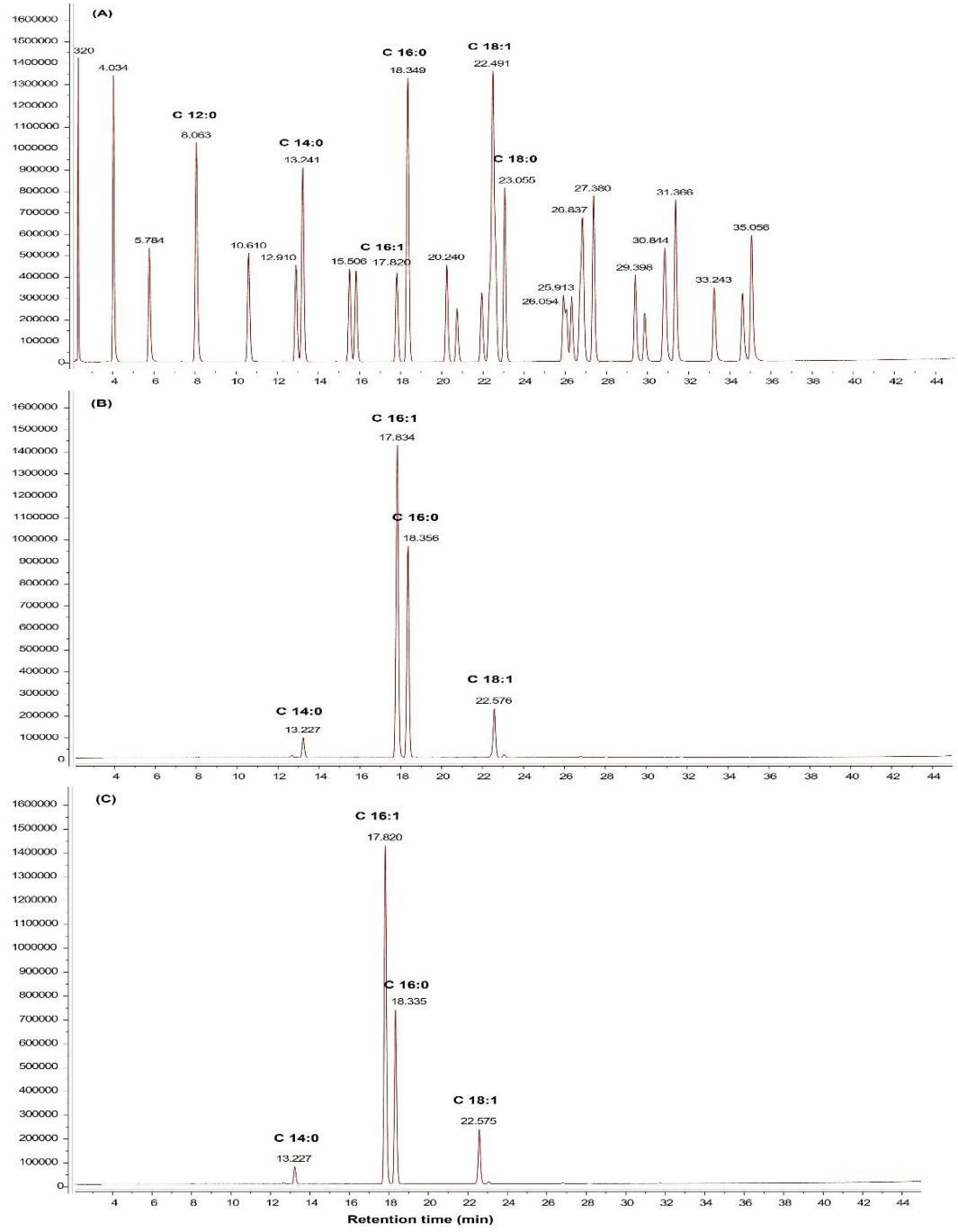

Figure 3.6 GC-MS analysis of (A) the FAME mix, (B) R3 and (C) R5 fatty acid chain profile.

Table 3.2 Fatty acid analysis of the native strains by GC-MS.

Retention time (min)	Fatty Acid chains	R3 (Mid-log)	R3 (Late-log)	R5 (Mid-log)	R5 (Late-log)
13.2	C14:0	3%	4%	3%	3%
18.3	C16:0	29%	30%	29%	28%
17.8	C16:1	50%	48%	51%	49%
22.5	C18:1	18%	18%	17%	20%
	Saturated/ Unsaturated	0.47	0.52	0.47	0.45

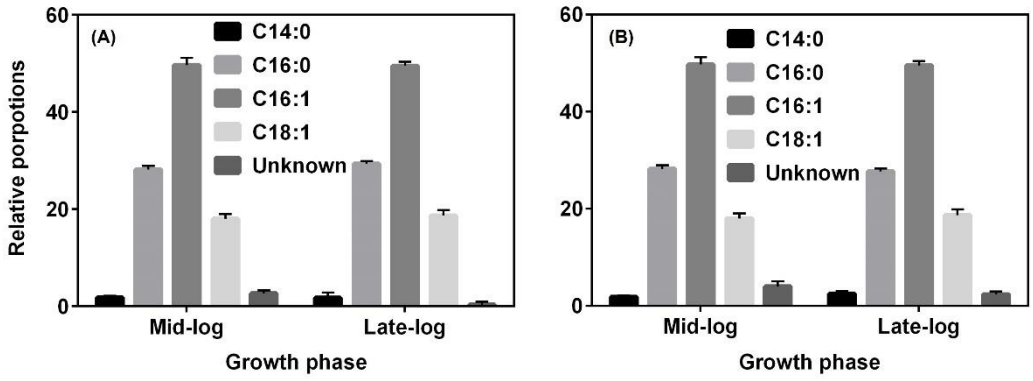

Figure 3.7 Fatty acid profile of (A) R3 and (B) R5 strains as determined by GC-MS.

3.3 Optimization of the labeling strategy

3.3.1 Detergent selection

Since FAs are generally insoluble in water, solubilizing exogenous Fas into detergent to form mixed micelles is necessary. The choice of a surfactant with a low CMC can be optimized by the growth curve observation and for prevention of cell disruption. Past publications from Marcotte's laboratory showed that different detergents are optimal, depending on the bacteria (Bouhlel *et al.*, 2019; Laadhari *et al.*, 2016; Tardy-

Laporte *et al.*, 2013). For example, DPC was found as the best surfactant to micellize PA for *E. coli*, while Tween-20 was less harmful towards *V. splendidus* (Bouhlel *et al.*, 2019; Laadhari *et al.*, 2016). Based on these previous publications, we have thus tested 0.15 mM of Tween-20 (CMC-0.06 mM) and 1 mM of DPC (CMC-1.5 mM) for mixed micelles formation with 0.1 mM of PA in a TSB culture medium. Considering the cost of deuterated fatty acids, we used protonated exogeneous FA acids for the detergent selection step. The structures of the detergents are presented in Figure 3.8.

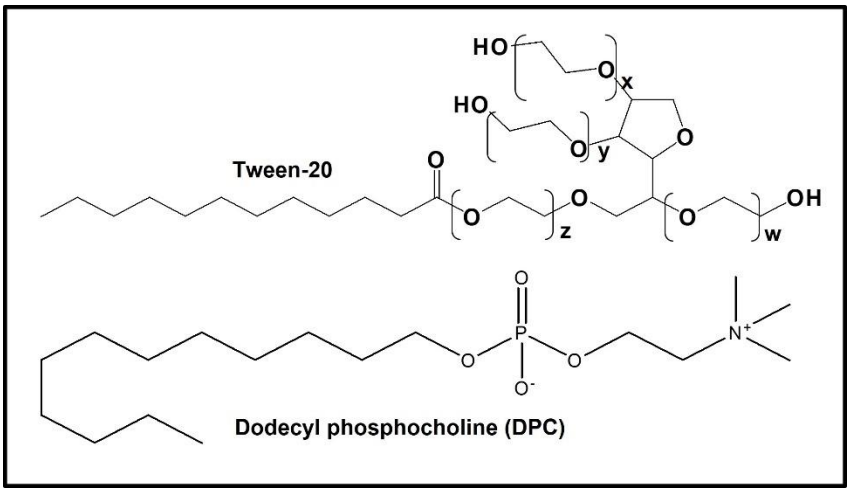

Figure 3.8 Molecular structures of dodecyl phosphocholine (DPC) and polyethylene glycol sorbitol monolaurate (Tween-20).

Figures 3.9 A and B show that the growth of R3 and R5 strains is less affected when 0.15 mM of Tween- 20 is used, thus more suitable for the labeling. Indeed, the growth curve obtained in the presence of Tween- 20 is almost the same as the one obtained with the native strains. Moreover, when 0.15 mM of Tween-20 is used without PA, the growth was also almost same as with PA in both strains (Figure 3.9). Tween In contrast, 1 mM of DPC with 0.1 mM of PA showed almost no growth after reaching an OD of 0.2-0.3. Therefore, DPC seems to be lethal for *A.s.s.* Therefore, 0.15 mM of Tween-20

is confirmed as the suitable detergent for our further experiments for the incorporation of FAs by both strains of *A.s.s* as in Figure 3.9.

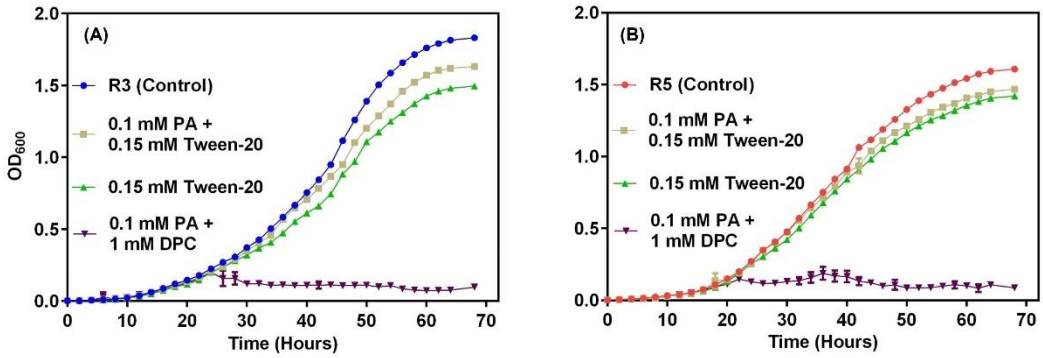

Figure 3.9 Determination of the detergent to be used for the micellization of the fatty acids. Growth curves of (A) R3 and (B) R5 were obtained at 18°C (PA- palmitic acid and DPC- dodecyl phosphocholine).

3.3.2 Optimization of the saturated-to-unsaturated FA chain molar ratio

We first started by adding 0.1 mM of POA micellized in 0.15 mM of Tween-20 to the culture medium. Tables 3.3 show that both strains of *A.s.s.* only minimally incorporated C16:1, from 46 to 54% in R3 and almost stable to 50% in R5 harvested in the late-log phase. When 0.1 mM of PA was used, a drastic increase in PA chains was observed as compared to the native strains. Indeed, the proportion of PA almost doubled when compared to the native strains. The SFA/UFA ratio increased to 1.86 in R3 and 1.50 in R5 from the native composition as shown in Tables 3.3. Finally, when OA was used, it was highly incorporated which was almost 4 times more than the native strains. Moreover, the composition of PA and POA was decreased to below 10%. Hence, the SFA/UFA ratio was consequently altered, dropping to 0.14. These results confirmed that the individual use of exogenous SFA or UFA altered the SFA/UFA ratio changing

the native individual FAs composition after labeling as shown in Table (3.3) and Figure 3.11.

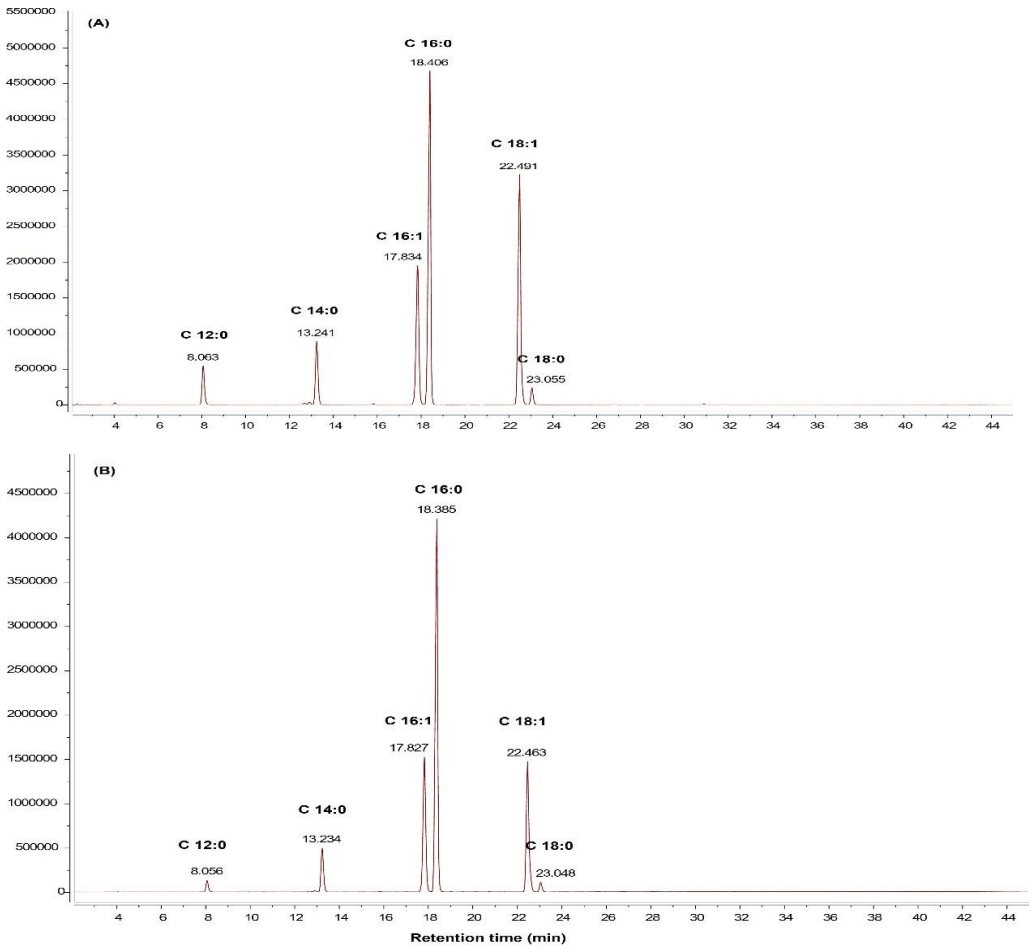

Figure 3.10 Fatty acid profile obtained by GC-MS for (A) R3 and (B) R5 strains grown in the presence of an equimolar ratio of OA and PA-d_{31} (0.1 mM).

Therefore, to maintain the SFA/UFA ratio as close as possible to the native *A.s.s.* strains, we used an equimolar concentration of OA or POA and PA (0.1 mM) micellized with Tween-20. The GC-MS results are shown in Figure 3.11 showed that there is the after addition of equimolar ratio of PA and POA, the value was almost same

to the value when only PA is added ad shown in Table (3.3) and Figure 3.11. Interestingly, although POA is naturally abundant in both strains, only the addition of OA restored the SFA/UFA ratio to an acceptable value of about 0.6 in both strains, and the incorporation was also efficient. All the results are summarized in Figure 3.11.

Table 3.3 Fatty acid chain profile of R3 as determined by GC-MS analysis, with and without addition of exogenous FAs in the growth medium and harvested in the late-log phase.

Retention time (min)	Fatty acid chains	R3 (Native)	PA	OA	POA	PA + POA	PA + OA
8.1	C12:0	-	3%	0%	2%	1%	3%
13.2	C14:0	4%	8%	4%	7%	6%	5%
18.3	C16:0	30%	53%	5%	22%	57%	30%
17.8	C16:1	48%	24%	6%	54%	28%	12%
22.5	C18:0	-	1%	3%	1%	2%	1%
23.1	C18:1	18%	11%	82%	14%	6%	49%
	Saturated/ Unsaturated	0.52	1.86	0.14	0.43	1.94	0.64

Table 3.4 Fatty acid chain profile of R5 as determined by GC-MS analysis, with and without addition of exogenous FAs in the growth medium and harvested in the late-log phase.

Retention time (min)	Fatty acid chains	R5 (Native)	PA	OA	POA	PA + POA	PA + OA
8.1	C12:0	**0**	**2%**	**0%**	**2%**	**0%**	**1%**
13.2	C14:0	3%	6%	5%	6%	3%	5%
18.3	C16:0	28%	50%	5%	27%	67%	31%
17.8	C16:1	49%	27%	6%	50%	23%	13%
22.5	C18:0	-	2%	2%	2%	1%	1%
23.1	C18:1	20%	13%	82%	13%	6%	49%
	Saturated/ Unsaturated	0.45	1.50	0.14	0.59	2.44	0.61

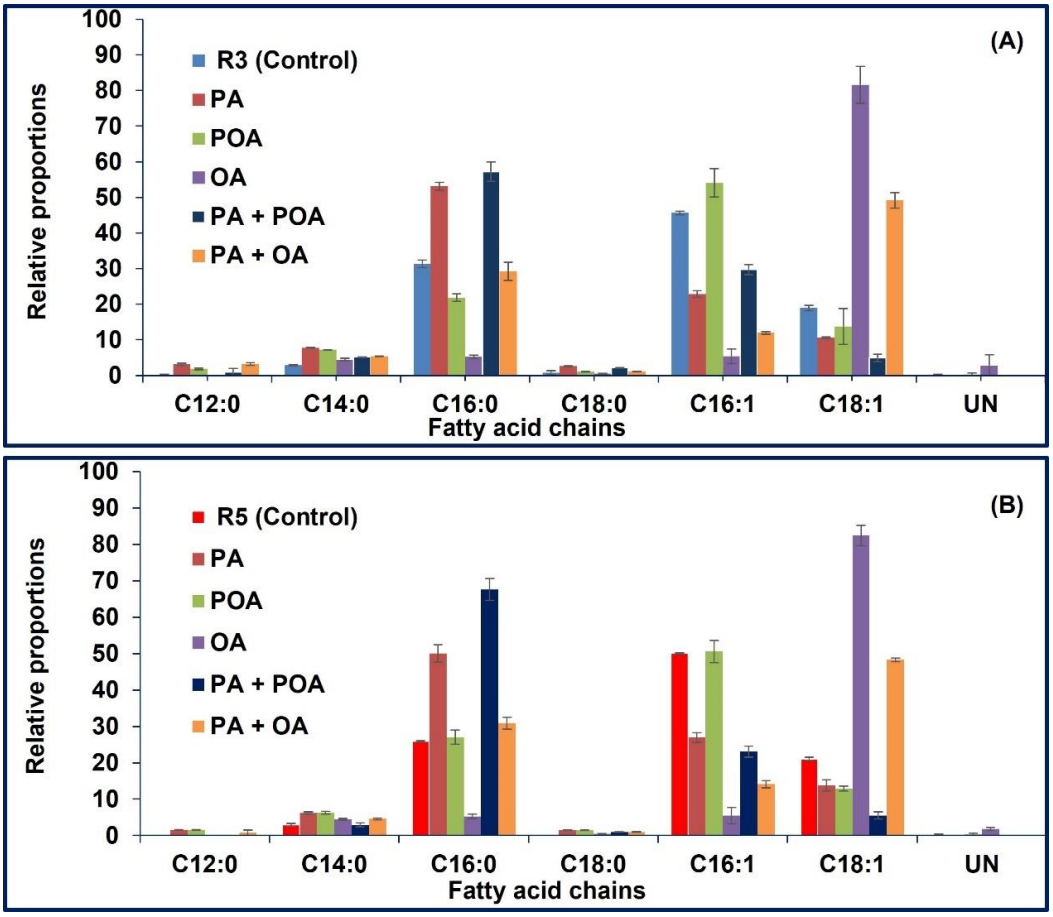

Figure 3.11 Fatty acid profile determined by GCMS of (A) R3 and (B) R5 grown in the presence of exogenous Fas and harvested in the late-log phase.

3.3.3 Deuterium labeling of *A.S.S.*

After establishing that an equimolar ratio of PA and OA (0.1 mM) micellized with 0.15 mM Tween-20 was suitable for deuterium labeling, we replaced the protonated PA with commercially available deuterated PA (PA-d_{31}). The labeled pellet was harvested in the late-log growth phase. A lipid extraction and GC-MS analysis were performed to verify the level of deuteration. As shown in Figure 3.12, the peak of the C16:1 and

C16:0-d_{31} overlap at the same retention time of 17.8 min and could not be separated under the GC-MS conditions used as shown in Figure 3.12.

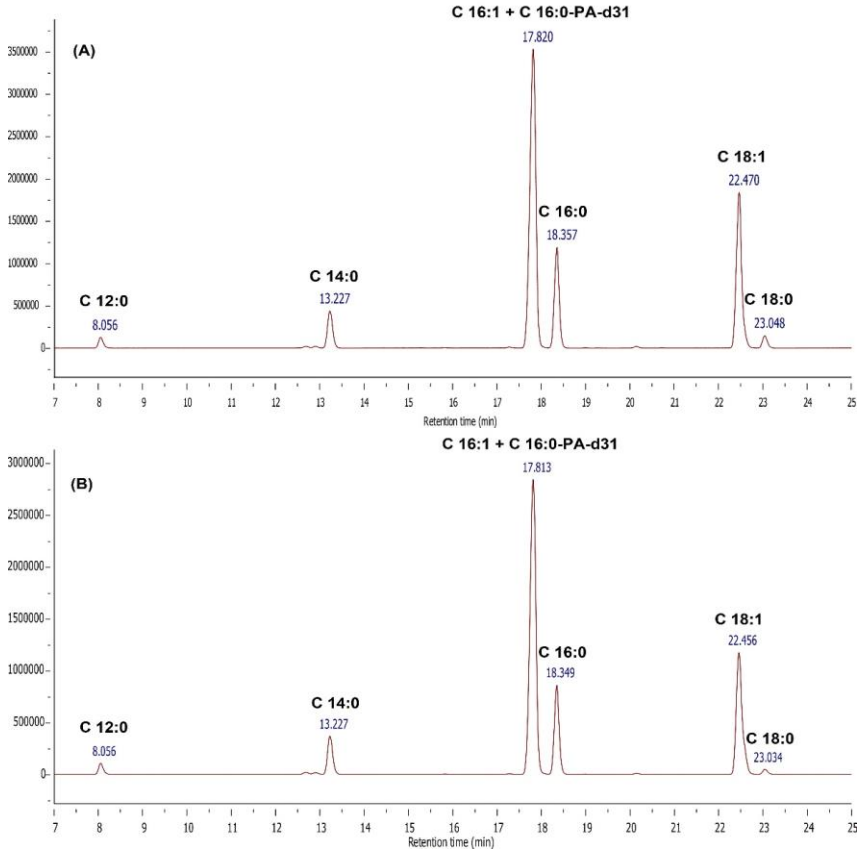

Figure 3.12 Fatty acid profile obtained by GCMS for (A) R3 and (B) R5 strains grown in the presence of an equimolar ratio of OA and PA-d_{31} (0.1 mM).

Therefore, to calculate the level of deuteration, we used the C16:1 value which is almost 12-13% of the overall FAs for both strains as a control, when protonated OA and PA are added to the culture medium from the section 3.3.2. Hence, we subtracted this C16:1 contribution in the deuterium labeled value and the remaining was assumed as being C16:0-d_{31}. The level of deuteration was found to be about 75-80% of the PA chains. This represented about 30% of all Fas (Table 3.5 and Figure 3.13). This value

is comparable to the deuteration of *V. splendidus* (31%) reported by Bouhlel *et al.* (Bouhlel *et al.*, 2019), and such level of deuteration allows a high S/N ratio for ^{2}H SS-NMR analysis.

Table 3.5. Level of deuteration analysis by GC-MS for both strains at late-log phase.

Retention time (min)	Fatty acid chains	R3 (Native)	R3 (PA-d31 + OA)	R5 (Native)	R5 (PA-d31 + OA)
8.1	C12:0	0%	2%	0%	1%
13.2	C14:0	4%	4%	3%	3%
18.3	C16:0	30%	5%	28%	6%
17.8	C16:0-d_{31}	0%	27%	0%	26%
17.8	C16:1	48%	12%	49%	13%
22.5	C18:1	18%	48%	20	49%
23.1	C18:0	-	1%	-	1%
	Unknown	0%	1%	0%	1%
	Saturated/ Unsaturated	0.52	0.64	0.45	0.59

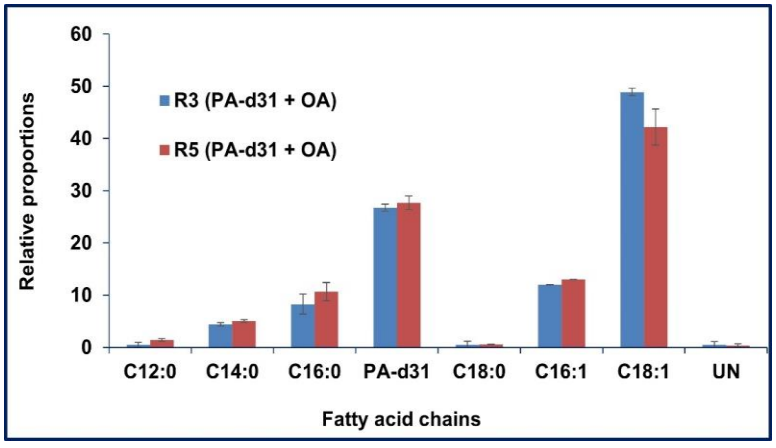

Figure 3.13 Fatty acid profile and deuteration level determined by GCMS of both *A.S.S.* strains grown in the presence of exogenous FAs and harvested in the late-log phase.

3.4 *In vivo* SS-NMR as a function of temperature

Static ^{2}HSS-NMR spectra are usually broad and long to acquire. However, with MAS probe, the broad spectrum is transformed into a narrow central peak with spinning sidebands, with increased sensitivity. With such spectrum, it is possible to deduce dynamic information: qualitatively, the more rigid the membrane is, the higher the number of sidebands. Increasing the temperature increases membrane dynamics, averages down the quadrupolar interaction, and is reflected by a reduction of the sideband intensities. Measuring the second spectral moment M_2 is a way to quantify these dynamic changes, as M_2 is related to the average order parameter as shown in Equation 1.3. On a ^{2}H SS-NMR spectrum, this is reflected by a reduction in the number of sidebands, and of the measured M_2 value, as shown in Figure 3.14. The value of M_2 was observed to be 37, 28 and 19 × $10^{9}s^{-2}$ at 8°C, 18°C and 28°C respectively the R3 strains. Similarly, the value of M_2 was observed as 35, 25 and 16 × $10^{9}s^{-2}$ at 8°C, 18°C and 28°C respectively in R5 strains as shown in Figure 3.15.

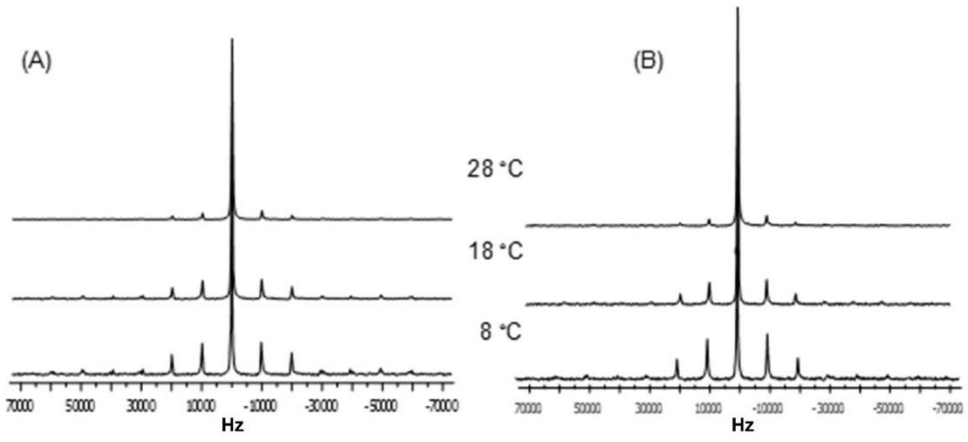

Figure 3.14 MAS (10 kHz) ^{2}H SS-NMR spectra of (A) R3 and (B) R5 acquired at 8°C, 18°C and 28°C with 4096 scans and 20 min of equilibrium time.

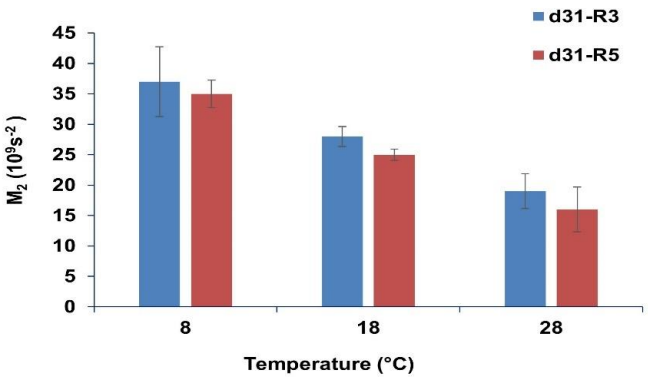

Figure 3.15 Graphical representation of the M_2 of R3 and R5 acquired at 8°C, 18°C and 28°C with 4096 and 20 min of equilibrium time.

3.5 Cell viability assay

A resazurin assay was performed for the determination of viable cells (R3 and R5) before and after NMR experiments. The samples were diluted to the OD_{600} of 0.1 with several dilutions (100%, 75%, 50% and 25%) before NMR as control. After 1 hour of reading of the fluorescence, the calibration graph was prepared, as shown in Figure 3.16 (A and B).

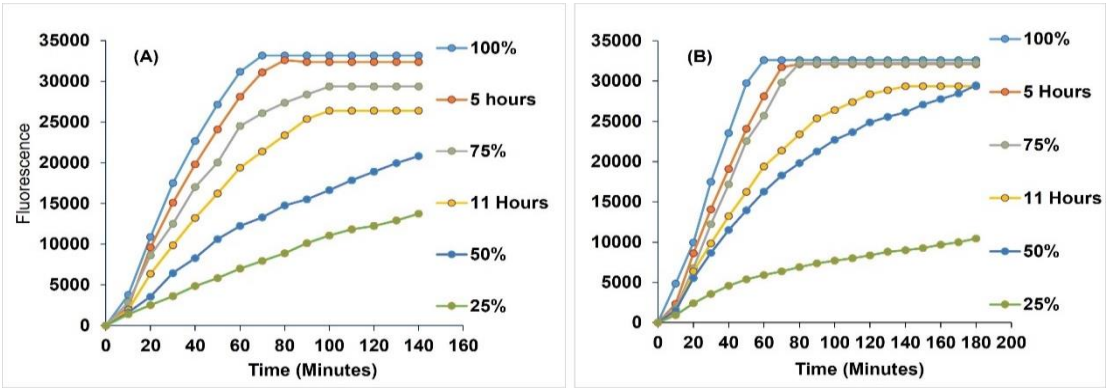

Figure 3.16 Resazurin assay calibration curve for cell viability of (A) R3 and (B) R5 with different dilution of the control sample without before NMR.

After immediate washing, 5 hours and 11 hours of the NMR experiments, the cell viability calibration curve was plotted as in Figures 3.16 (A and B). Cell viability was calculated using equation 2.1 after one hour of incubation. The viability after washing was above 95%, while a viability of 90% was determined after 5 hours of NMR experiments, and superior to 50% after 11 hours, for both strains as shown in Figure 3.17 (A and B).

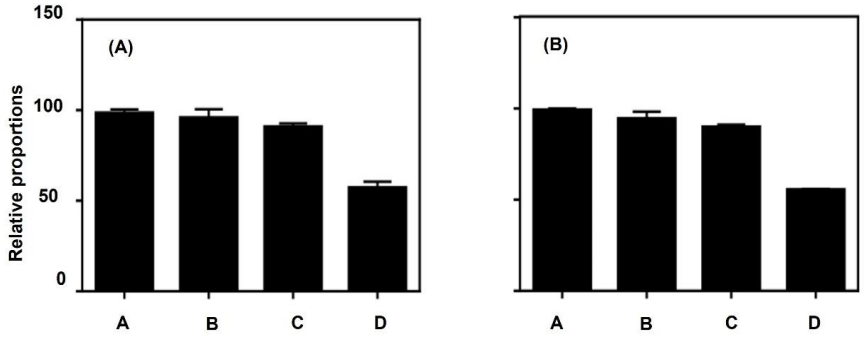

Figure 3.17 Cell viability of (A) R3 and (B) R5 at different time intervals before and after NMR (A = control; B = non-deuterated after washing; C = after 5 hours of NMR; D = after 11 hours of NMR).

3.6. MIC and MBC assay

We determined the minimum inhibitory concentration (MIC) and minimum bactericidal concentration (MBC) of two antibiotics against both strains of *A.s.s* by serial dilution and OD_{600} measurement. The MIC was determined to be 1 μg/mL for both antibiotics, as shown in Figure 3.18.

MBC determination was made by taking the two samples above the MIC and one sample below the MIC of the antibiotics, and inoculated in the TSB plates, including the positive control. The TSB plates were incubated at 18° C for 72 hours. The MBC was also determined to be 1 μg/mL for both antibiotics, as shown in Figure 3.19.

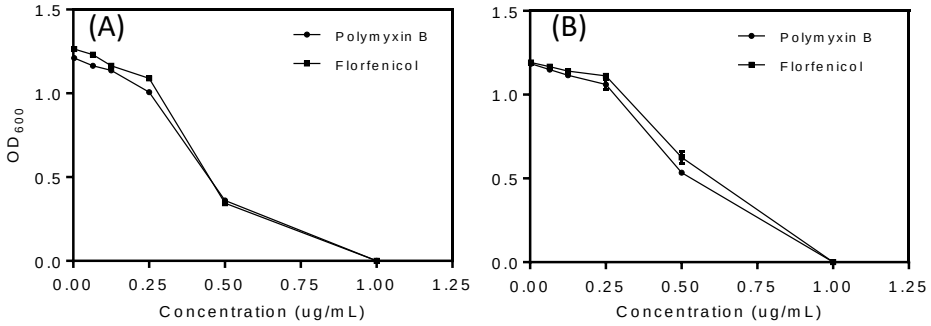

Figure 3.18 MIC assay of polymyxin-B and Florfenicol against (A) R3 and (B) R5.

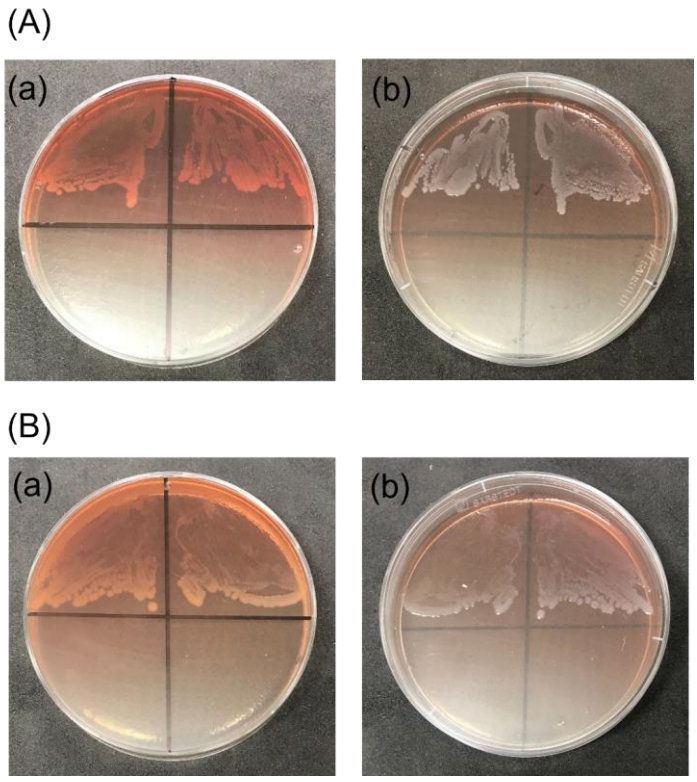

Figure 3.19 MBC assay of (A) polymyxin-B and (B) florfenicol against (a) R3 and (b) R5. Visible growth observed on 0.5µg/mL and control. No growth observed on 1 µg/mL and 2 µg/mL for both antibiotics.

CHAPTER IV

DISCUSSION

Aeromonas salmonicida subspecies *salmonicida* is known as a universal threat to salmons and trout with a diseased condition called furunculosis. The various virulent properties exhibited by this bacterium are responsible for a high mortality rate in the fish industry. Moreover, *A.s.s.* develops resistance against different antibiotics. It is evident that antimicrobial agents must cross the membrane of any bacterium to exert their mechanism of action and kill those harmful bacteria. Therefore, the main objective of our project was to establish a new isotopic labeling strategy and perform a biophysical characterization of *A.s.s.* by ^{2}H SS-NMR *in vivo* to enable the study of the interaction of membranes with antibiotics in future works. Moreover, we used strains with (R3) and without (R5) an A-layer, which will allow investigating the role of this layer in the action mechanism.

4.1 Establishing the ^{2}H-labeling protocol

In this work, we showed for the first time the successful ^{2}H-labeling of *A.s.s.* membranes with deuterated exogenous FAs for both strains. We first determined that the optimal growth temperature of both *A.s.s.* strains is 18°C. In comparison, *E. coli* and the marine bacterium *V. splendidus* respectively grow at 25°C and 37°C (Bouhlel *et al.*, 2019). However, the growth temperature is an important factor for any bacteria for the optimal growth. *E. coli* is a fast growing bacterium, and can reach the stationary phase after 6-8 hours when in a favorable growth medium at room temperature (Laydevant *et al.*, 2022). On the contrary, *A.s.s.* is a slow-growing bacterium as it takes

48-50 hours to reach the exponential phase, when *V. splendidus* needs half this time *(*Bouhlel *et al.,* 2019*). A* reduced OD at the plateau for R5 compared to R3 at each growth temperature, as shown in Figure 3.2, can be assigned to the lack of A-layer which would make R5 more sensitive towards external conditions.

We were also able to determine the lipid head group portrait of both *A.s.s.* strains by ^{31}P solution NMR. Interestingly, both strains showed an identical phospholipid head group profile in which PE dominates (78-80%) followed by PG (12-15%) and CL (3%-5%) (Figure 3.5). Interestingly, *A.s.s.* phospholipidic profile is similar to *E. coli* (75% PE, 15-20% PG, and 4-5% CL) and *V. splendidus* (80-85% PE, 10-15% PG, 4-5% CL), which are all gram-negative (Bouhlel *et al.*, 2021; Warnet *et al.*, 2016).

The native FAs composition of both strains was then studied by GC-MS to determine the dominant FAs present in the bacteria as well as the SFA/UFA ratio that must be targeted in the ^{2}H-labeling protocol. Results displayed in Table 3.2, are relatively similar to previous data reported in the literature for the same bacterium (Bektas *et al.*, 2007; Morgan *et al.,* 1991). However, it was observed that the OA composition was higher in *A.s.s*. Bektas *et al.* harvested the cell after 48 hours and the subspecies was not specified. In contrast, we harvested the cells after 54 to 60 hours. In addition, GC-MS is a quantitative analytical method that requires the determination of a correction factor for each fatty acid. In our hands, the only significant correction factor was that of OA, which was determined to be 2.52, based on measurement done on a commercial FAME mix, as shown in APPENDIX D. The discrepancy between literature results and ours may come from their forgetting to take this correction factor into account (Bektas *et al.*, 2007).

Interestingly, the FA composition of R3 and R5 is almost identical in both the mid-and late-log phases (Table 2.2). When compared to other Gram negative bacteria, we can note that the FAs composition of *A.s.s.* is very similar to that of another marine bacterium, *V. splendidus,* in which POA (C16:1) is dominant (~50% of overall FAs),

followed by PA (C16:0, ~30%) (Bouhlel *et al.*, 2019). In *E. coli*, the most abundant FA chains are PA (~40-45%) and OA (~30-40%) and POA is absent (Laydevant *et al.*, 2022).

The previous labeling protocols established in the Marcotte laboratory, we improved the selection of detergent and found 0.15 mM of Tween-20 in 300 mL of TSB to be suitable for mixed micelle formation. This is similar to the labeling protocol published for *V. splendidus* (Bouhlel *et al.*, 2019). Considering that POA, FA chains were dominating in both R3 and R5 strains, we used C16:1 as our first choice for labeling. However, we only observed the proportion of C16:1 to increase by ~8%, at the expense of C16:0 (Tables 3.3 and 3.4, Figure 3.11). In previous successful bacterial labeling, FA incorporation exceeded 30% (Bouhlel *et al.*, 2019; Laydevant *et al.*, 2022), allowing a good S/N ratio by ^{2}H SS-NMR. POA labeling in *A.s.s.* is therefore not very efficient. When the bacteria were grown in the presence of both POA and PA in equimolar ratio, a drastic increase in C16:0 was observed in both strains. PA's proportion was almost doubled as compared to the native strains, resulting in an alteration of the SFA/UFA ratio (from 0.4 to almost 2). These results could be due to the lack of incorporation of POA, or to the modification of POA after its incorporation. For example, C16:1 would be turned into C16:0, elongated into C18:1, further unsaturated into C16:2, shortened to C14:0, or even cyclopropanated into cyC17:0 (David Giles and Steven Symes, The University of Tennessee at Chattanooga, Private Communication). The FA monitoring in both strains showed no increase in the abundance of these possible FA chains. It thus appears that both strains do not incorporate C16:1, although it can incorporate C16:0 alone, or C16:0 and C18:1 together in an equimolar ratio. We can postulate that the very high natural occurrence of C16:1 acyl chain has reached a threshold and that A.S.S. cannot incorporate any more exogenous C16:1 (David Giles and Steven Symes, The University of Tennessee

at Chattanooga, Private Communication). The low integration of POA in A.S.S. deserves to be investigated.

When only PA was used in the growth medium, a successful incorporation occurred, but the SFA/UFA ratio drastically changed, and was almost quadrupled, from 0.52 to 1.86 in R3 and 0.45 to 1.56 in R5 (Tables 3.3 and 3.4, Figure 3.11), as already observed in different bacterial species (Bouhlel *et al.*, 2019; Tardy-Laporte *et al.*, 2013; Warnet *et al.*, 2016). This increases the membrane rigidity, despite the adaptive change of bacteria in various temperatures (Weber *et al.*, 2001). The SFA/UFA ratio was similar to the native one for both strains when PA-d_{31} and OA were added in the growth medium at equimolar ratio (Tables 3.3 and 3.4, Figure 3.11), corresponding to the labeling strategy used with *E. coli* and *V. splendidus* (Bouhlel *et al.*, 2019). Our GC-MS analysis showed that 75-80% of the PA acyl chains were deuterated in the membranes, representing that 25-30% of overall FAs acyl chains (Table 3.5 and Figure 3.13). This level of deuteration was higher than the labeling reached with *V. splendidus* (69%) (Bouhlel *et al.*, 2019). Hence, we labeled both *A.s.s.* strains (R3 and R5) with PA-d_{31} in the presence of protonated OA in equimolar ratio, micellized in Tween-20 and at 18°C.

4.2 *In vivo* ^{2}H SS-NMR analysis and changes in dynamics

In-cell SS-NMR is a powerful and non-invasive technique for studying the lipids dynamics and their interaction with various extracellular molecules (proteins, antibiotics, antimicrobial peptides, etc.) (Booth, 2021; Laadhari *et al.*, 2016; Tardy-Laporte *et al.*, 2013). The successful application of MAS to *in vivo* ^{2}H SS-NMR studies opened up a new era in the NMR field (Warnet *et al.*, 2016). Indeed, the sensitivity was thus increased, and the acquisition time of the spectra was significantly less than static SS-NMR, facilitating the study of ^{2}H-labeled bacterial and their interaction with AMPs. The deuteration level of the bacterial membrane played a significant role for acquiring high-resolution ^{2}H SS-NMR spectra.

Our results show that more than 90% of the cells were viable after 5 hours in the spectrometer, and 60% of the bacteria were still alive after 11 hours of continuous NMR experiments (Figure 3.17 A and B). The calibration curve showed that the presence of the A-layer in R3 might play a protective role for the dye to get inside the cell as compared to R5 (Figures 2.16 A and B). The initial viability of the native cells and the deuterated cells were almost the same. The viability of the bacteria decreased to below 60% after 11 hours of NMR experiments. The viability determined with the two *A.S.S.* strains is comparable that of *V. splendidus* after labeling and NMR experiments (Bouhlel *et al.*, 2019).

It was known that the virulence properties of *A.s.s.* decrease with an increase in temperature (Ishiguro *et al.*, 1981; Wiklund, 1995). Also, the dynamics of labeled bacterial membranes increase with the temperature (Bouhlel *et al.*, 2019; Warnet *et al.*, 2016). Therefore, monitoring the change in lipid dynamics of the bacteria as a function of temperature is a way to verify that the labeling was successfully achieved. The calculation of M_2 allowed quantifying the change of fluidity (rigid or fluid) of labeled membranes. The decrease in M_2 values observed for both strains with an increase in temperature indicates that the bacteria are properly labeled. The M_2 values are similar to those obtained with *V. splendidus* but also with pure deuterated dipalmitoyl phosphatidylcholine (DPPC-d_{62}) (Warnet *et al.*, 2015). Therefore, our results show that *A.s.s.* strains ^{2}H-labeled using our protocol are suitable to monitor the effects of antibiotics on bacterial membranes by *in vivo* ^{2}H SS-NMR.

We chose two potent antibiotics against *A.s.s.* because of their mode of action for killing bacteria. Florfenicol kills the bacteria by disrupting the protein synthesis, whereas Polymyxin B interacts with the Gram-negative bacteria membranes. We will assess the membrane effect of Polymyxin B and Florfenicol against both strains of labeled *A.s.s* by *in vivo* ^{2}H SS-NMR. We determined the MIC values of these

antibiotics, and these values will be further used to prepare our samples for *in vivo* ^{2}H SS-NMR. We will use concentrations below, above and at the MIC for the interaction.

This future project could possibly set a new milestone to understand the role of the A-layer in the interaction between both antibiotics and bacterial membranes, by comparing the labeled lipid acyl chains dynamics on both strains. The A-layer may play a role in preventing the interaction of antimicrobial agents with labeled membranes, and comparing labeled R3 and R5 strains may thereby help us learn more about this process. However, both these strains are not natural strains, they are mutants created by heat stress, which lack T3SS for laboratory use (Paquet *et al.*, 2019). Therefore, it will also be necessary to understand the possible different mechanism between wild-type and mutated strains.

Labeling the cell membrane is the first step in our biophysical characterization of the bacterial cell. However, the scope is still limited because many antibiotics have other targets than the cell membrane. The presence of the A-layer in the wild-type strain is known to play a significant role for protection against different enzymes and bacteriophages (Paquet *et al.*, 2019) (Kay et Trust, 1991; Rollauer *et al.*, 2015). Therefore, while all the experiments and results presented in this project aim to characterize the cell membrane after isotopic labeling, labeling the A-layer would allow us to directly probe the interaction of antibiotics with this important barrier. In summary, there is still more research to be done to understand *A.s.s.* virulence and pathogenicity and its resistance to antibiotics, and we hope that *in vivo* SS-NMR can help contribute to this ongoing research.

CONCLUSION AND PERSPECTIVES

A.s.s. is renowned for threatening salmonids aquaculture since it is a causative agent for furunculosis. Its built-in virulent properties and antibiotic-resistant gene development create a huge challenge to deal within fish farming. The presence of A-layer, T3SS systems and different plasmids conferring resistance to various antibiotics make it more lethal. The roles of the A-layer which acts as the first defensive barrier for this bacterium against different antibacterial agents are still under research. Ongoing research also aims to better understand the virulence properties of the A-layer, Lipid A, LPS, etc.

However, in consideration of this pathogenic bacterium and its continuous pathological attributes, and for the need to understand the action of membrane disrupting antibiotics and antimicrobial peptides, we proposed a successful ^{2}H-labeling strategy for *in vivo* ^{2}H SS-NMR investigation. This provides a solid foundation to better understand changes in membrane dynamics. Furthermore, it opens the door for labeling protocol development with different isotopes (^{13}C, ^{19}F, etc.). Such labeling could be notably useful to measure distances between an antibiotic agent and the lipids, which would help mapping the insertion. In this work, the successful isotopic membrane labeling of *A.s.s.* (R3 and R5) allowed us to understand the change of dynamics as a function of temperature, indicating that antimicrobial agent interactions can be further studied by SS-NMR, *in vivo*. The stress shown by the bacterial species with labeling can also be studied. Finally, the choice of two strains with (R3) and without A-layer (R5) allows to probe the role of this outer layer on membrane properties by NMR.

The establishment of this labeling strategy opens new avenues with different research perspectives. Nevertheless, we have already started to explore the changes in labeled

membrane dynamics after the interaction of different antibiotics used against *A.s.s*. The limited incorporation of POA is also an interesting finding during this project. For biologists, exploring the role of POA in *A.S.S* membranes and verifying the mechanism behind the low incorporation of exogenous POA could also be a new research perspective.

This project mainly focused on labeling the cell membrane, but labeling the different cell wall layers (LPS, PGN, Lipid A and A-layer) will possibly give us more information about the antibiotic's interaction with Gram negative bacteria. For instance, polymyxin B kills Gram negative bacteria by disrupting the LPS. If we could establish the labeling protocol for LPS then the exact LPS disruption mechanism could also be verified in the future, likewise for protein. We could even explore the exact interaction of labeled membranes with labeled antibiotics or AMPs by Rotational-Echo DOuble-Resonance (REDOR) by measuring the distance between the labeled membrane and antimicrobial agent. Moreover, our findings and establishment of a labeling strategy for *A.S.S.* is not only useful for verifying interaction mechanism of antibiotics but also with AMPs, probiotics, bacteriophages, etc., by ^{2}H SS-NMR, *in vivo.*

APPENDIX A

CULTURE MEDIA PREPARATION

Tryptic soy broth/agar media preparation (TSB/TSA, 1 liter of nanopure water)

Materials

- Tryptone (pancreatic digest of casein) – 17.0 g
- Soytone (peptic digest of soyabean) – 3 g
- Dextrose – 2.5 g
- Sodium chloride – 5 g
- Dipotassium phosphate- 2.5 g

Procedure

- Mix all the above ingredients in 1000 ml of nanopure water.
- Heat to boiling to dissolve the medium completely.
- Sterilize by autoclaving at 15 lbs pressure (121°C) for 15 min.
- Cool the sterile medium to room temperature before use.
- For TSA plates, add 15 g of agar and autoclave as above.
- Cool to 45-50°C.
- Mix well and pour into sterile Petri plates.
- Let plates with hot medium cool down and seal the plates.
- Store the plates at 4°C.

Note: CBB agar is prepared by adding 0.01% of Coomassie brilliant blue R-250 to tryptic soy agar.

Inoculation of the *A.s.s.* culture

- Add 10-20 ml of TSB to a tube or flask.
- Using a sterile inoculation loop, select a single colony from the TSA plate.
- Mix well the inoculum in the medium.
- Incubate the tube/ flask at 18°C at 200 rpm for 48-72 hours.
- After incubation, the sample is ready for stock culture preparation or experiments.

Preparation of stock culture

- Prepare the 50% glycerol solution by diluting 100% glycerol in nanopure water.
- After observing bacterial growth, add 500 µL of the overnight culture to 500 µL of 50% glycerol in a 2 mL Eppendorf tube and mix gently.
- Freeze the glycerol stock tube at -80°C. The stock is now stable for years if it is kept at -80°C.

Furunculosis Agar medium preparation (1 liter)

Materials

- Bacto-Tryptone- 10 g
- Yeast extract- 5 g
- L-tyrosine- 1 g
- NaCl- 2.5 g
- Agar- 15 g

Procedure

- Mix all the above compounds in 1000 ml of nanopure water.
- Heat to boiling to dissolve the medium completely.

- Sterilize by autoclaving at 15 lbs pressure (121°C) for 15 min.
- For TSA plates, add 15 g of agar and autoclave as above.
- Cool to 45-50°C.
- Mix well and pour into sterile Petri plates.
- Take a loopful of bacterial culture from the stock culture with a sterile loop.
- Streak the inoculum culture into the furunculosis agar (FA) plates.
- Incubate the plates at 18°C for 3-4 days for the pigmentation to appear.

Coomassie Brilliant Blue Agar Preparation (1 liter)

Materials

- Bacto-Tryptone- 10 g
- Yeast extract- 5 g
- L-tyrosine- 1 g
- NaCl- 2.5 g
- Agar- 15 g

Procedure

- Mix all the above compounds in 1000 ml of nanopure water.
- Heat to boiling to dissolve the medium completely.
- Sterilize by autoclaving at 15 lbs. pressure (121°C) for 15 min.

APPENDIX B

FATTY ACID MICELLES PREPARATION

Preparation of exogenous FA micelles:

Procedure:

- Prepare the right amount of PA (7.7 mg of PA or 8.6 mg of PA-d_{31}) and dissolve in 4 mL of methanol in a 15 mL Falcon tube.
- Evaporate the methanol with a nitrogen stream to obtain a PA film on the tube.
- Evaporate the last traces of methanol with the vacuum pump.
- Add the right amount of Tween-20 (55.2 mg).
- Add 10 mL of TSB medium (the mixture may not be clear).
- Heat to 95°C for 5 min in a closed tube.
- Vortex for 1 minute.
- Cool in liquid nitrogen for 5 min in a closed tube.
- Repeat *steps 6-8* three more times (so a total of four times).

  (At this point, PA should be solubilized by Tween-20 micelles, but it could be unstable.)
- Heat to 50°C for 5 min in a closed tube. The solution should be transparent. Wait for 5 min at room temperature and check for the appearance of small PA crystals. If they appear, again repeat heat, and freeze cycle twice.

- Add bacterial preculture that correspond to 0.1 OD in 290 ml of TSB. Pour the warm 10 mL solution of PA/Tween-20/TSB, PA/DPC/TSB, and Tween-20/TSB into 290 mL of bacterial culture.
- Take OD at zero hour. Incubate the flask at 18^{o}C at 200 rpm.
- Aliquot 1 ml of the culture suspension at an interval of every 2 hours and take the optical density (OD) at a wavelength of 600 nm using spectrophotometer, until the reading becomes static.
- At the end of the experiment, plot a graph of the OD_{600} as a function of time, to obtain the growth curve of bacteria.

APPENDIX C

LIPID AND FATTY ACIDS ANALYSIS

Lipid extraction preparation:

- KCl solution (0.88%): 0.88 g of KCl in 100 ml of nanopure water.
- Dichloromethane (DCM)- methanol solution (2:1): 50 ml of DCM and 25 ml of methanol/ sample.

Protocol:

- Wash the bacteria pellet with 0.9% saline solution and centrifuge at 4200 rpm for 10 min to remove the supernatant (repeat this step 3-4 times).
- The mass of the wet pellet of culture is approximately 200-300 mg at mid-log and 400-500 mg at late-log phase for 300 mL culture for 36- and 50-hours growth phase, respectively.
- Wash the pellet with 5 ml nanopure water and centrifuge at above.
- Lyophilize the bacterial pellet overnight. The dry pellet is approximately 30-50 and 90-100 mg of weight from mid log and late-log growth phase of wet pellet from 300 ml culture media, respectively.

Lipid extraction protocol (Folch):

- Transfer the pellet to a 50 ml glass vial.
- In a graduated cylinder, measure 50 ml of DCM-methanol (2:1) solution.
- Add 25 ml of the solvent to the 50 mL glass vial with the pellet and vortex to dissolve it.

- Sonicate the bacterial pellet at 8W on the ice bath for 1 min. (Repeat this process for 3 times with 1 minute of interval and vortex).
- Transfer the sample to the separating funnel and add remaining 25 mL of solvent to the separating funnel.
- Shake vigorously for 2 min and degas to release the pressure.
- Let it stand for 10-15 min.
- Add 14 mL of 0.88% KCl solution to the mixture.
- Shake vigorously for 2 min and degas to release the pressure.
- Let it stand for 10-15 min for the phase separation.
- If the organic phase is not cloudy (bottom), filter this phase. If it remains cloudy, add a few mL of DCM-methanol solution.
- Weigh 5 mL empty vial for the lipid storage.
- Collect and evaporate the organic phase of the 5 mL stored vial under a stream of nitrogen at 40°C.
- Add 2-3 mL of DCM-methanol solution to the flask to recover the lipids again in the separating funnel.
- Once completely dried, place the vial in the freeze dryer for 30-45 min.
- Weigh the dry mass of lipids and store them in the refrigerator at 4°C (1.5-2.5 mg of lipids at mid log and 3-5 mg of lipids at late-log phase for 300 mL, respectively.

^{31}P solution NMR sample preparation:

- Collect the lyophilized vial with lipid and add 500 µL of deuterated chloroform + 200 µL of methanol and 50 µL of EDTA (pH 6.0 with H_2O).
- Vortex and transfer the sample to NMR tubes.
- Seal the tube with the plugs and vortex and the tubes are ready for lipid analysis by ^{31}P solution NMR.

Fatty Acid Analysis by GC-MS:

Methylation:

- Preparation of MeOH solution (1 mL H_2SO_4 + 49 mL MeOH)
- Remove the upper phase of EDTA with a Pasteur pipette and evaporate any solvent under nitrogen at 40°C.
- In vial: add 2 mL solution MeOH + 0.8 mL toluene and close the sample under nitrogen.
- Heat the sample to 100°C degassing and vortex from time to time for 10 min.
- Cool to room temperature for 10 min and transfer the sample into a glass centrifuge flask.
- In a centrifugation vial: add 4 mL distilled water + 0.8mL hexane.
- Centrifuge at 2000 rpm for 2 min at 22°C.
- Take the upper organic layer and discard the other layer.
- Evaporate upper organic layer vial with nitrogen at 40°C.
- Lyophilize (if there is any aqueous layer present in the sample) the vial for 30 min prepares for GC-MS

Fatty acid analysis by GC-MS: Preparation of the samples and FAME (C4-C24) mix:

FAME mix prepared in hexane:

- Sample preparation for GC-MS
- In vial: 0.5 ml hexane
- Add insert in vial of GC-MS
- Use syringe and filter to filter sample into the insert
- Close the vial with cap.

APPENDIX D

SUPPLEMENTARY RESULTS

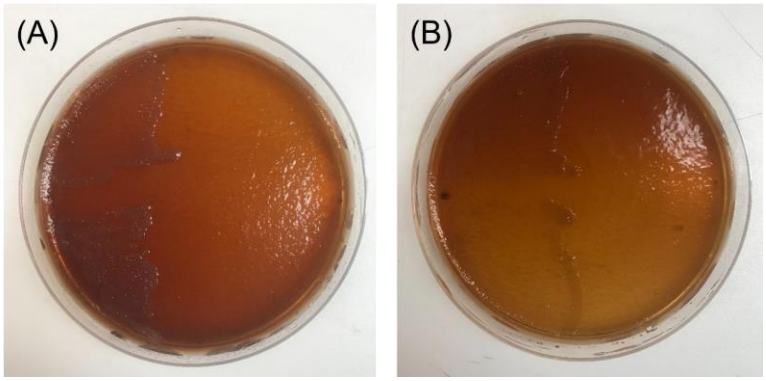

Figure 6.1 Colony differentiation of (A) R3 and (B) R5. R3 forms dark brownish buttery colony while R5 colonies was light brownish.

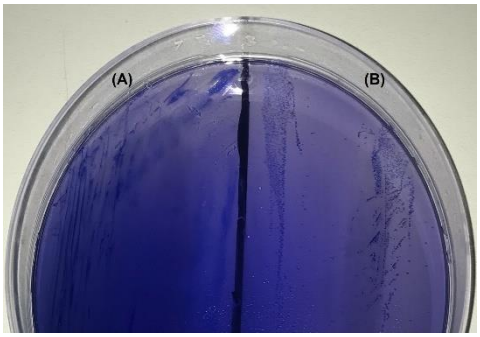

Figure 6.2 CBB plates showing the presence of A-layer. (A) R3 absorbs the brilliant blue pigment, while (B) R5 remains non-pigmented (Paquet *et al.*, 2019).

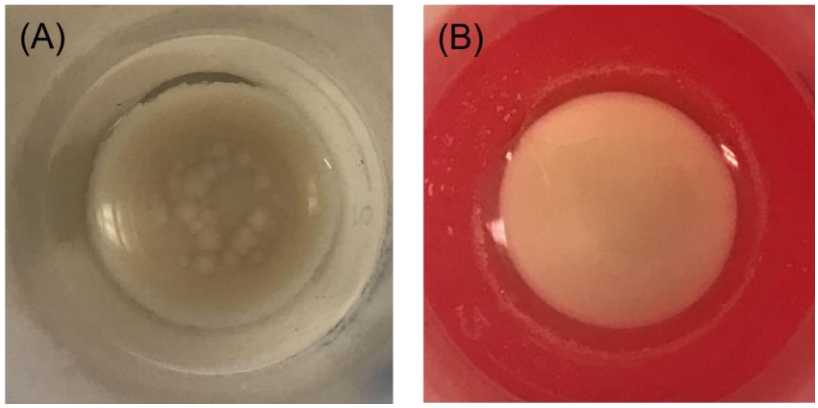

Figure 6.3 Distinctive rough surface of (A) R3 and plain surface of (B) R5 pellets after centrifugation.

Table 6.1 ^{31}P chemical shift of lipid hear groups after labeling.

Strain	PG	CL	PE
R3	0.65	0.40	0.08
R5	0.65	0.39	0.08

Table 6.2 Lipid head group profile of both strains of *A.s.s* .after labeling.

Strain	PE	PG	CL
R3	78	14	4
R5	79	13	4

Table 6.3. FAME analysis by GC-MS and correction factor determination

Retention time (min)	Area	Molecular weight	Hit Name	FAs (%)	Industrial (%)	Correction factor
2.228	328130	186.198	1-Octanol, 2-butyl-	-	-	-
2.327	38708440	158.131	Octanoic acid, methyl ester	2.76	3.99	0.54
4.041	68164902	186.162	Decanoic acid, methyl ester	4.86	4	0.95
5.784	36162433	200.178	Undecanoic acid, methyl ester	2.6	2	1.02
8.07	77509716	214.193	Dodecanoic acid, methyl ester	5.52	3.99	1.08
10.61	39612640	228.209	Tridecanoic acid, methyl ester	2.82	2	1.1
12.91	36797313	240.209	Methyl Z-11-tetradecenoate	2.62	1.99	1.03
13.241	72432528	242.225	Methyl tetradecanoate	5.16	4.02	1
15.513	34751014	282.256	Cyclopropaneoctanoic acid, 2-hexyl-, methyl ester	2.47	2	0.96
15.831	34224370	256.24	Pentadecanoic acid, methyl ester	2.44	1.99	0.96
17.813	33957266	268.24	9-Hexadecenoic acid, methyl ester, (Z)-	2.42	2	0.95
18.349	104770258	270.256	Hexadecanoic acid, methyl ester	7.46	5.99	0.97
20.24	35198138	282.256	Cyclopropaneoctanoic acid, 2-hexyl-, methyl ester	2.51	2	0.98
20.741	19690550	284.272	Heptadecanoic acid, methyl ester	1.41	1.17	0.95
21.941	26534087	292.24	6,9,12-Octadecatrienoic acid, methyl ester	1.89	2	0.74
22.491	181357839	296.272	11-Octadecenoic acid, methyl ester	12.92	4	2.52
23.062	62576372	298.287	Octadecanoic acid, methyl ester	4.46	3.99	0.87
25.92	25847444	332.272	5,8,11,14-Eicosatetraenoic acid, ethyl ester, (all-Z)-	1.84	2	0.72
26.054	17458370	316.24	5,8,11,14,17-Eicosapentaenoic acid, methyl ester, (all-Z)-	1.21	1.48	0.64
26.315	25495516	320.272	5,8,11-Eicosatrienoic acid, methyl ester	1.82	2.01	0.71
26.837	84088832	324.303	11-Eicosenoic acid, methyl ester	5.99	4.01	1.17
27.38	62336079	326.318	Eicosanoic acid, methyl ester	4.44	2	1.73
29.405	33290732	340.334	Heneicosanoic acid, methyl ester	2.37	1.71	1.08
29.871	19336681	342.256	4,7,10,13,16,19-Docosahexaenoic acid, methyl ester, (all-Z)-	1.38	1.99	0.54
30.844	57408097	236.214	Z,Z-10,12-Hexadecadienal	4.09	2	1.6
31.366	62150772	354.35	Docosanoic acid, methyl ester	4.43	3.99	0.87
33.243	30907757	368.365	Tricosanoic acid, methyl ester	2.2	1.7	1
34.626	29136158	380.365	15-Tetracosenoic acid, methyl ester	2.08	2	0.81
35.063	53461974	382.381	Tetracosanoic acid, methyl ester	3.81	3.99	0.43

BIBLIOGRAPHY

Adams C, Austin B, Meaden P *et* McIntosh D (1998) Molecular characterization of plasmid-mediated oxytetracycline resistance in *Aeromonas salmonicida*. *Applied and Environmental Microbiology, 64*: 4194-4201.

Alanis AJ (2005) Resistance to antibiotics: are we in the post-antibiotic era? *Archives of Medical Research, 36*: 697-705.

Ambaye A, Kohner PC, Wollan PC, Roberts KL, Roberts GD *et* Cockerill 3rd F (1997) Comparison of agar dilution, broth microdilution, disk diffusion, E-test, and BACTEC radiometric methods for antimicrobial susceptibility testing of clinical isolates of the *Nocardia asteroides* complex. *Journal of Clinical Microbiology, 35*: 847-852.

Andersson DI, Balaban NQ, Baquero F, Courvalin P, Glaser P, Gophna U, Kishony R, Molin S *et* Tønjum T (2020) Antibiotic resistance: turning evolutionary principles into clinical reality. *FEMS Microbiology Reviews, 44*: 171-188.

Andrew E, Bradbury A *et* Eades R (1958) Nuclear magnetic resonance spectra from a crystal rotated at high speed. *Nature, 182*: 1659-1659.

Andrew ER (1981) Magic angle spinning in solid-state NMR spectroscopy. *Philosophical Transactions of the Royal Society of London Series A, Mathematical and Physical Sciences, 299*: 505-520.

Antonoplis A, Zang X, Wegner T, Wender PA *et* Cegelski L (2019) Vancomycin–arginine conjugate inhibits growth of carbapenem-resistant *E. coli* and targets cell-wall synthesis. *American Chemical Society, Chemical Biology, 14*: 2065-2070.

Aoki T, Egusa S, Kimura T *et* Watanabe T (1971) Detection of R factors in naturally occurring *Aeromonas salmonicida* strains. *Applied Microbiology, 22*: 716-717.

Aoki T, Egusa S, Yada C *et* Watanabe T (1972) Studies of Drug Resistance and R Factors in Bacteria from Pond-Cultured Salmonids: I. Amago (*Oncorhynchus rhodurus macrostomus)* and Yamame (*Oncorhynchus masou ishikawae*). *Japanese Journal of Microbiology, 16*: 233-238.

Austin B, Austin DA *et* Munn C (2007) Bacterial fish pathogens: disease of farmed and wild fish. Springer, United Kingdom.

Barton BA *et* Iwama GK (1991) Physiological changes in fish from stress in aquaculture with emphasis on the response and effects of corticosteroids. *Annual Review of Fish Diseases, 1*: 3-26.

Bektas S, Ayik O *et* Yanik T (2007) Fatty acid profile and antimicrobial susceptibility of *Aeromonas salmonicida* isolated from rainbow trout. *International Journal of Pharmacology, 3*: 191-194.

Benveniste R *et* Davies J (1973) Mechanisms of antibiotic resistance in bacteria. *Annual Review of Biochemistry, 42*: 471-506.

Bernoth E-M (1997) Furunculosis: the history of the disease and of disease research. Dans *Furunculosis*. Elsevier, San Diego, California, 1-20.

Bhat RAH, Thakuria D, Pant V, Khangembam VC, Tandel RS, Shahi N, Sarma D, Tripathi G, Krishnani KK *et* Krishna G (2020) Antibacterial and antioomycete activities of a novel designed RY12WY peptide against fish pathogens. *Microbial Pathogenesis, 149*: 104591.

Booth V (2021) Deuterium Solid State NMR studies of intact bacteria treated with antimicrobial peptides. *Frontiers in Medical Technology, 2*: 621572.

Bouhlel Z, Arnold AA, Warschawski DE, Lemarchand K, Tremblay R *et* Marcotte I (2019) Labelling strategy and membrane characterization of marine bacteria *Vibrio splendidus* by in vivo ^{2}H NMR. *Biochimica et Biophysica Acta-Biomembranes, 1861*: 871-878.

Boyd JM, Dacanay A, Knickle LC, Touhami A, Brown LL, Jericho MH, Johnson SC *et* Reith M (2008) Contribution of type IV pili to the virulence of *Aeromonas salmonicida* subsp. salmonicida in Atlantic salmon (*Salmo salar L*.). *Infection and Immunity, 76*: 1445-1455.

Brenner DJ, Krieg NR, Staley JT *et* Garrity G (2005) *Bergey's Manual® of Systematic Bacteriology: Volume two the Proteobacteria part C The Alpha-, Beta-, Delta-, and Epsilonproteobacteria*. Springer, New York.

Burnett L *et* Muller B (1971) Deuteron quadrupole coupling constants in three solid deuterated paraffin hydrocarbons: C2D6, C4D10, C6D14. *The Journal of Chemical Physics, 55*: 5829-5831.

Burr SE, Stuber K, Wahli T *et* Frey J (2002) Evidence for a type III secretion system in *Aeromonas salmonicida* subsp. *salmonicida*. *Journal of Bacteriology 184*: 5966-5970.

Byers DM *et* Gong H (2007) Acyl carrier protein: structure–function relationships in a conserved multifunctional protein family. *Biochemistry and Cell Biology, 85*: 649-662.

Chu S, Cavaignac S, Feutrier J, Phipps B, Kostrzynska M, Kay W *et* Trust T (1991) Structure of the tetragonal surface virulence array protein and gene of *Aeromonas salmonicida*. *Journal of Biological Chemistry, 266*: 15258-1526.

Cipriano RC *et* Bertolini J (1988) Selection for virulence in the fish pathogen *Aeromonas salmonicid*a, using Coomassie Brilliant Blue agar. *Journal of Wildlife Diseases, 24*: 672-678.

Cipriano RC *et* Bullock GL (2001) Furunculosis and other diseases caused by *Aeromonas salmonicida*. *Fish Disease Leaflet, 66*.

Coleman G *et* Whitby PW (1993) A comparison of the amino acid sequence of the serine protease of the fish pathogen *Aeromonas salmonicida* subsp. *salmonicida* with those of other subtilisin-type enzymes relative to their substrate-binding sites. *Microbiology, 139*: 245-249.

Cornelis GR *et* Van Gijsegem F (2000) Assembly and function of type III secretory systems. *Annual Reviews in Microbiology, 54*: 735-774.

Daher RK, Filion G, Tan SGE, Dallaire-Dufresne S, Paquet VE *et* Charette SJ (2011) Alteration of virulence factors and rearrangement of pAsa5 plasmid caused by the growth of *Aeromonas salmonicida* in stressful conditions. *Veterinary Microbiology, 152*: 353-360.

Dallaire-Dufresne S, Tanaka KH, Trudel MV, Lafaille A *et* Charette SJ (2014) Virulence, genomic features, and plasticity of *Aeromonas salmonicida* subsp. *salmonicida*, the causative agent of fish furunculosis. *Veterinary Microbiology, 169*: 1-7.

Davis JH (1979) Deuterium magnetic resonance study of the gel and liquid crystalline phases of dipalmitoyl phosphatidylcholine. *Biophysical Journal, 27*: 339-358.

Davis JH, Nichol CP, Weeks G *et* Bloom M (1979) Study of the cytoplasmic and outer membranes of *Escherichia coli* by deuterium magnetic resonance. *Biochemistry, 18*: 2103-2112.

Ellis A, Burrows A *et* Stapleton K (1988) Lack of relationship between virulence of *Aeromonas salmonicida* and the putative virulence factors: A-layer, extracellular proteases, and extracellular haemolysins. *Journal of Fish Diseases, 11*: 309-323.

Estrada R, Stolowich N *et* Yappert MC (2008) Influence of temperature on ^{31}P NMR chemical shifts of phospholipids and their metabolites I. In chloroform–methanol–water. *Analytical Biochemistry, 380*: 41-50.

Etebu E *et* Arikekpar I (2016) Antibiotics: Classification and mechanisms of action with emphasis on molecular perspectives. *International of Journal Applied Microbiology and Biotechnology Research, 4*: 90-101.

Folch J, Lees M *et* Sloane Stanley GH (1957) A simple method for the isolation and purification of total lipids from animal tissues. *The Journal of Biological Chemistry, 226*: 497-509.

Frey J *et* Origgi FC (2016) Type III secretion system of *Aeromonas salmonicida* undermining the host's immune response. *Frontiers in Marine Science, 3*: 130.

Fryer J, Rohovec J, Tebbit G, McMichael J *et* Pilcher K (1976) Vaccination for control of infectious diseases in Pacific salmon. *Fish Pathology, 10*: 155-164.

Garduño RA, Moore AR, Olivier G, Lizama AL, Garduño E *et* Kay WW (2000) Host cell invasion and intracellular residence by *Aeromonas salmonicida*: role of the S-layer. *Canadian Journal of Microbiology, 46*: 660-668.

Griffin P, Snieszko S *et* Friddle S (1953) A new adjuvant in the diagnosis of fish furunculosis caused by bacterium *salmonicida*. *Veterinary Medicine, 48*: 280-282.

Gulla S, Lund V, Kristoffersen A, Sørum H *et* Colquhoun D (2016) vapA (A-layer) typing differentiates *Aeromonas salmonicida* subspecies and identifies a number of previously undescribed subtypes. *Journal of Fish Diseases, 39*: 329-342.

Hancock RE *et* Scott MG (2000) The role of antimicrobial peptides in animal defenses. *Proceedings of The National Academy of Sciences, 97*: 8856-8861.

Hasan TH *et* Al-Harmoosh RA (2020) Mechanisms of antibiotics resistance in bacteria. *Systemic Reviews in Pharmacy, 11*: 817-823.

Hennel JW *et* Klinowski J (2005) Magic-angle spinning: a historical perspective. Dans *New Techniques in Solid-State NMR*. Springer, Berlin, Heidelberg, *Topics in Current Chemistry, 246*: 1-14.

Hotinger JA *et* May AE (2020) Antibodies inhibiting the type III secretion system of Gram-negative pathogenic bacteria. *Antibodies, 9*: 35.

Huang KC, Mukhopadhyay R, Wen B, Gitai Z *et* Wingreen NS (2008) Cell shape and cell-wall organization in Gram-negative bacteria. *Proceedings of the National Academy of Sciences, 105*: 19282-19287.

Imbeault S, Parent S, Lagacé M, Uhland CF *et* Blais J-F (2006) Using bacteriophages to prevent furunculosis caused by *Aeromonas salmonicida* in farmed brook trout. *Journal of Aquatic Animal Health, 18*: 203-214.

Ishiguro E, Kay W, Ainsworth T, Chamberlain J, Austen R, Buckley J *et* Trust T (1981) Loss of virulence during culture of *Aeromonas salmonicida* at high temperature. *Journal of Bacteriology, 148*: 333-340.

Janda JM *et* Abbott SL (2010) The genus *Aeromonas*: taxonomy, pathogenicity, and infection. *Clinical Microbiology Reviews, 23*: 35-73.

Kay W, Buckley J, Ishiguro E, Phipps B, Monette J *et* Trust T (1981) Purification and disposition of a surface protein associated with virulence of *Aeromonas salmonicida. Journal of Bacteriology, 147*: 1077-1084.

Kay W *et* Trust T (1991) Form and functions of the regular surface array (S-layer) of *Aeromonas salmonicida*. *Experientia, 47*: 412-414.

Kowalska-Krochmal B *et* Dudek-Wicher R (2021) The minimum inhibitory concentration of antibiotics: Methods, interpretation, clinical relevance. *Pathogens, 10*: 165.

Kumar K, Sebastiao M, Arnold AA, Bourgault S, Warschawski DE *et* Marcotte I (2022) *In situ* solid-state NMR study of antimicrobial peptide interactions with erythrocyte membranes. *Biophysical Journal,* 9;121(8):1512-1524.

L'Abée-Lund TM *et* Sørum H (2000) Functional Tn 5393-like transposon in the R plasmid pRAS2 from the fish pathogen *Aeromonas salmonicida* subspecies *salmonicida* isolated in Norway. *Applied and Environmental Microbiology, 66*: 5533-5535.

Laadhari M, Arnold AA, Gravel AE, Separovic F *et* Marcotte I (2016) Interaction of the antimicrobial peptides caerin 1.1 and aurein 1.2 with intact bacteria by ^{2}H solid-state NMR. *Biochimica et Biophysica Acta-Biomembranes, 1858*: 2959-2964.

Lara-Tejero M *et* Galán JE (2019) The injectisome, a complex nanomachine for protein injection into mammalian cells. *EcoSal Plus, 8(2)*: 10.1128.

Laydevant F, Mahabadi M, Llido P, Bourgouin J-P, Caron L, Arnold AA, Marcotte I *et* Warschawski DE (2022) Growth-phase dependence of bacterial membrane lipid profile and labeling for in-cell solid-state NMR applications. *Biochimica et Biophysica Acta-Biomembranes, 1864*: 183819.

Lee K *et* Ellis A (1990) Glycerophospholipid: cholesterol acyltransferase complexed with lipopolysaccharide (LPS) is a major lethal exotoxin and cytolysin of *Aeromonas salmonicida*: LPS stabilizes and enhances toxicity of the enzyme. *Journal of Bacteriology, 172*: 5382-5393.

Lowe I (1959) Free induction decays of rotating solids. *Physical Review Letters, 2*: 285.

Maricq MM *et* Waugh JS (1979) NMR in rotating solids. *The Journal of Chemical Physics, 70*: 3300-3316.

Marques TV, Paschoal JAR, Barone RSC, Cyrino JEP *et* Rath S (2018) Depletion study and estimation of withdrawal periods for florfenicol and florfenicol amine in pacu (*Piaractus mesopotamicus*). *Aquaculture Research, 49*: 111-119.

Marr AG *et* Ingraham JL (1962) Effect of temperature on the composition of fatty acids in *Escherichia coli*. *Journal of Bacteriology, 84*: 1260-1267.

Massicotte M-A, Vincent AT, Schneider A, Paquet VE, Frenette M *et* Charette SJ (2019) One *Aeromonas salmonicida* subsp. *salmonicida* isolate with a pAsa5 variant bearing antibiotic resistance and a pRAS3 variant making a link with a swine pathogen. *Science of the Total Environment, 690*: 313-320.

Meng L, Du Y, Liu P, Li X *et* Liu Y (2017) Involvement of LuxS in *Aeromonas salmonicida* metabolism, virulence, and infection in Atlantic salmon (*Salmo salar L*). *Fish & Shellfish Immunology, 64*: 260-269.

Midtlyng PJ (1997) Vaccination against furunculosis. Dans *Fish Vaccination*, Wiley, Chapter 16: 185-199.

Midtlyng PJ (2016) Methods for measuring efficacy, safety, and potency of fish vaccines. Dans *Fish vaccines*. Springer, Basel, 119-141.

Morgan J, Cranwell P *et* Pickup R (1991) Survival of Aeromonas salmonicida in lake water. *Applied and Environmental Microbiology, 57*: 1777-1782.

Munn C, Ishiguro E *et* Kay W (1982) Role of surface components in serum resistance of virulent *Aeromonas salmonicida*. *Infection and Immunity, 36*: 1069-1075.

Nikaido H (2009) Multidrug resistance in bacteria. *Annual Review of Biochemistry, 78*: 119.

Oldfield E, Chapman D *et* Derbyshire W (1971) Deuteron resonance: a novel approach to the study of hydrocarbon chain mobility in membrane systems. *Federation of European Biochemical Societies Letters, 16*: 102-104.

Oldfield E, Keough K *et* Chapman D (1972) The study of hydrocarbon chain mobility in membrane systems using spin-label probes. *Federation of European Biochemical Societies Letters, 20*: 344-346.

Paquet VE, Vincent AT, Moineau S *et* Charette SJ (2019) Beyond the A-layer: adsorption of lipopolysaccharides and characterization of bacteriophage-insensitive mutants of *Aeromonas salmonicida* subsp. *salmonicida*. *Molecular microbiology 112*: 667-677.

Paracini N, Schneck E, Imberty A *et* Micciulla S (2022) Lipopolysaccharides at the interface. *Advances in Colloid and Interface Science,* 102603.

Pius J, Morrow MR *et* Booth V (2012) ^{2}H solid-state nuclear magnetic resonance investigation of whole *Escherichia coli* interacting with antimicrobial peptide MSI-78. *Biochemistry, 51*: 118-125.

Riss TL, Moravec RA, Niles AL, Duellman S, Benink HA, Worzella TJ *et* Minor L (2016) Cell viability assays. Dans *Assay Guidance Manual.* Eli Lilly &Company for Advancing Translational Sciences, Bethesda, NBK144065.

Rodgers C (1990) Immersion vaccination for control of fish furunculosis. *Diseases of Aquatic Organisms, 8*: 69-72.

Rodríguez-Melcón C, Alonso-Calleja C, García-Fernández C, Carballo J *et* Capita R (2021) Minimum inhibitory concentration (MIC) and minimum bactericidal concentration (MBC) for twelve antimicrobials (biocides and antibiotics) in eight strains of *Listeria monocytogenes*. *Biology*, *11*: 46.

Rollauer SE, Sooreshjani MA, Noinaj N *et* Buchanan SK (2015) Outer membrane protein biogenesis in Gram-negative bacteria. *Philosophical Transactions of the Royal Society B: Biological Sciences, 370*: 20150023.

Salton M (1953) Studies of the bacterial cell wall: IV. The composition of the cell walls of some Gram-positive and Gram-negative bacteria. *Biochimica et Biophysica acta, 10*: 512-523.

Santisteban NP, Morrow MR *et* Booth V (2017) Protocols for studying the interaction of MSI-78 with the membranes of whole Gram-positive and Gram-negative bacteria by NMR. *Methods in Molecular Biology, 1548*: 217-230.

Seelig J *et* Macdonald PM (1987) Phospholipids and proteins in biological membranes. Deuterium NMR as a method to study structure, dynamics, and interactions. *Accounts of Chemical Research, 20*: 221-228.

Serber Z, Keatinge-Clay AT, Ledwidge R, Kelly AE, Miller SM *et* Dötsch V (2001) High-resolution macromolecular NMR spectroscopy inside living cells. *Journal of the American Chemical Society, 123*: 2446-2447.

Silhavy TJ, Kahne D *et* Walker S (2010) The bacterial cell envelope. *Cold Spring Harbor Perspectives in Biology, 2*: a000414.

Sleytr UB, Schuster B, Egelseer E-M *et* Pum D (2014) S-layers: principles and applications. *Federation of European Microbiological Societies, Microbiology Reviews, 38*: 823-864.

Sohlenkamp C *et* Geiger O (2016) Bacterial membrane lipids: diversity in structures and pathways. *Federation of European Microbiological Societies, Microbiology Reviews, 40*: 133-159.

Sørum H, L'Abée-Lund TM, Solberg A *et* Wold A (2003) Integron-containing IncU R plasmids pRAS1 and pAr-32 from the fish pathogen *Aeromonas salmonicida*. *Antimicrobial Agents and Chemotherapy, 47*: 1285-1290.

Stockton GW, Johnson KG, Butler KW, Tulloch A, Boulanger Y, Smith IC, DAVIS JH *et* BLOOM M (1977) Deuterium NMR study of lipid organisation in *Acholeplasma laidlawii* membranes. *Nature, 269*: 267-268.

Tardy-Laporte C, Arnold AA, Genard B, Gastineau R, Morançais M, Mouget J-L, Tremblay R *et* Marcotte I (2013) A ^{2}H solid-state NMR study of the effect of antimicrobial agents on intact *Escherichia coli* without mutating. *Biochimica et Biophysica Acta-Biomembranes, 1828*: 614-622.

Trudel MV, Vincent AT, Attéré SA, Labbé M, Derome N, Culley AI *et* Charette SJ (2016) Diversity of antibiotic-resistance genes in Canadian isolates of *Aeromonas salmonicida* subsp. *salmonicida*: dominance of pSN254b and discovery of pAsa8. *Scientific Reports, 6*: 35617.

Vincent AT, Hosseini N *et* Charette SJ (2021) The *Aeromonas salmonicida* plasmidome: A model of modular evolution and genetic diversity. *Annals of the New York Academy of Sciences, 1488*: 16-32.

Wang Z, Li J, Vinogradov E *et* Altman E (2006) Structural studies of the core region of *Aeromonas salmonicida* subsp. *salmonicida* lipopolysaccharide. *Carbohydrate Research, 341*: 109-117.

Warnet XL, Arnold AA, Marcotte I *et* Warschawski DE (2015) *In-cell* solid-state NMR: an emerging technique for the study of biological membranes. *Biophysical Journal, 109*: 2461-2466.

Warnet XL, Laadhari M, Arnold AA, Marcotte I *et* Warschawski DE (2016) A ^{2}H magic-angle spinning solid-state NMR characterisation of lipid membranes in intact bacteria. *Biochimica et Biophysica Acta-Biomembranes, 1858*: 146-152.

Warschawski DE, Arnold AA, Beaugrand M, Gravel A, Chartrand É *et* Marcotte I (2011) Choosing membrane mimetics for NMR structural studies of

transmembrane proteins. *Biochimica et Biophysica Acta-Biomembranes, 1808*: 1957-1974.

Weber MH, Klein W, Müller L, Niess UM *et* Marahiel MA (2001) Role of the *Bacillus subtilis* fatty acid desaturase in membrane adaptation during cold shock. *Molecular Microbiology, 39*: 1321-1329.

Wiegand I, Hilpert K *et* Hancock RE (2008) Agar and broth dilution methods to determine the minimal inhibitory concentration (MIC) of antimicrobial substances. *Nature Protocols, 3*: 163-175.

Wiklund T (1995) Survival of' atypical' *Aeromonas salmonicida* in water and sediment microcosms of different salinities and temperatures. *Diseases of Aquatic Organisms, 21*: 137-143.

Wiklund T *et* Dalsgaard I (1998) Occurrence and significance of atypical *Aeromonas salmonicida* in non-salmonid and salmonid fish species: a review. *Diseases of Aquatic Organisms, 32*: 49-69.

Zhang Y-M *et* Rock CO (2008) Membrane lipid homeostasis in bacteria. *Nature Reviews Microbiology, 6*: 222-233.